REPORT

Biallelic Variants in *OTUD6B* Cause an Intellectual Disability Syndrome Associated with Seizures and Dysmorphic Features

Teresa Santiago-Sim,[1,2,27] Lindsay C. Burrage,[1,3,27] Frédéric Ebstein,[4] Mari J. Tokita,[1,2] Marcus Miller,[1,2] Weimin Bi,[1,2] Alicia A. Braxton,[1,2] Jill A. Rosenfeld,[1] Maher Shahrour,[5] Andrea Lehmann,[4] Benjamin Cogné,[6] Sébastien Küry,[6] Thomas Besnard,[6] Bertrand Isidor,[6,7] Stéphane Bézieau,[6] Isabelle Hazart,[8] Honey Nagakura,[9] LaDonna L. Immken,[9] Rebecca O. Littlejohn,[10] Elizabeth Roeder,[1,10] EuroEPINOMICS RES Consortium Autosomal Recessive working group, S. Hande Caglayan,[11] Bulent Kara,[12] Katia Hardies,[13,14] Sarah Weckhuysen,[13,14,15] Patrick May,[16] Johannes R. Lemke,[17] Orly Elpeleg,[18] Bassam Abu-Libdeh,[5] Kiely N. James,[19] Jennifer L. Silhavy,[19] Mahmoud Y. Issa,[20] Maha S. Zaki,[20] Joseph G. Gleeson,[19] John R. Seavitt,[1] Mary E. Dickinson,[1,21] M. Cecilia Ljungberg,[22,23] Sara Wells,[24] Sara J. Johnson,[24] Lydia Teboul,[24] Christine M. Eng,[1,2] Yaping Yang,[1,2] Peter-Michael Kloetzel,[4,25] Jason D. Heaney,[1,26,28,*] and Magdalena A. Walkiewicz[1,2,28,*]

Ubiquitination is a posttranslational modification that regulates many cellular processes including protein degradation, intracellular trafficking, cell signaling, and protein-protein interactions. Deubiquitinating enzymes (DUBs), which reverse the process of ubiquitination, are important regulators of the ubiquitin system. *OTUD6B* encodes a member of the ovarian tumor domain (OTU)-containing subfamily of deubiquitinating enzymes. Herein, we report biallelic pathogenic variants in *OTUD6B* in 12 individuals from 6 independent families with an intellectual disability syndrome associated with seizures and dysmorphic features. In subjects with predicted loss-of-function alleles, additional features include global developmental delay, microcephaly, absent speech, hypotonia, growth retardation with prenatal onset, feeding difficulties, structural brain abnormalities, congenital malformations including congenital heart disease, and musculoskeletal features. Homozygous *Otud6b* knockout mice were subviable, smaller in size, and had congenital heart defects, consistent with the severity of loss-of-function variants in humans. Analysis of peripheral blood mononuclear cells from an affected subject showed reduced incorporation of 19S subunits into 26S proteasomes, decreased chymotrypsin-like activity, and accumulation of ubiquitin-protein conjugates. Our findings suggest a role for OTUD6B in proteasome function, establish that defective OTUD6B function underlies a multisystemic human disorder, and provide additional evidence for the emerging relationship between the ubiquitin system and human disease.

Whole-exome sequencing (WES) has proven powerful for discovering new genes associated with genetically heterogeneous disorders, including global developmental delay, intellectual disability, and seizures.[1–4] In our clinical WES cohort of roughly 9,000 unrelated individuals, the majority of whom have neurologic manifestations and belong to the pediatric age group, we identified two unrelated individuals with biallelic variants in *OTUD6B* (MIM: 612021) with overlapping clinical features. Through GeneMatcher,[5] we subsequently identified 10 additional individuals, yielding a total of 12 affected subjects from 6 unrelated families (Figure 1). We obtained written informed consent from all study participants in accordance with protocols approved by institutional review boards at Baylor College of Medicine (USA), University of Kiel (Germany), National Research Center (Egypt), CHU de Nantes (France), and Makassed Islamic Charitable Hospital (Jerusalem).

[1]Department of Molecular and Human Genetics, Baylor College of Medicine, Houston, TX 77030, USA; [2]Baylor Miraca Genetics Laboratories, Baylor College of Medicine, Houston, TX 77021, USA; [3]Texas Children's Hospital, Houston, TX 77030, USA; [4]Charité-Universitätsmedizin Berlin, Institute of Biochemistry, Charité Platz 1/Virchowweg 6, 10117 Berlin, Germany; [5]Department of Pediatrics and Genetics, Makassed Hospital and Al-Quds University, Jerusalem 91220, Palestine; [6]CHU de Nantes, Service de Génétique Médicale, Nantes Cedex 1 44093, France; [7]INSERM, UMR-S 957, 1 Rue Gaston Veil, Nantes 44035, France; [8]CHU de Nantes, Service de Pédiatrie, Nantes Cedex 1 44093, France; [9]Specially for Children, Austin, TX 78723, USA; [10]Department of Pediatrics, Baylor College of Medicine, San Antonio, TX 78207, USA; [11]Department of Molecular Biology and Genetics, Bogazici University, Istanbul 34342, Turkey; [12]Department of Pediatrics, Kocaeli University Medical Faculty, Kocaeli 41380, Turkey; [13]Neurogenetics Group, Center of Molecular Neurology, VIB, Antwerp 2610, Belgium; [14]Laboratory of Neurogenetics, Institute Born-Bunge, University of Antwerp, Antwerp 2610, Belgium; [15]Division of Neurology, Antwerp University Hospital, Antwerp 2610, Belgium; [16]Luxembourg Centre for Systems Biomedicine, University of Luxembourg, Esch-sur-Alzette 4362, Luxembourg; [17]Institute of Human Genetics, University of Leipzig Hospitals and Clinics, 04103 Leipzig, Germany; [18]Monique and Jacques Roboh Department of Genetic Research, Hadassah-Hebrew University Medical Center, Jerusalem 91120, Israel; [19]Laboratory for Pediatric Brain Disease, Howard Hughes Medical Institute, Department of Neurosciences, University of California, San Diego, CA 92093, USA; [20]Clinical Genetics Department, Human Genetics and Genome Research Division, National Research Centre, Cairo 12311, Egypt; [21]Department of Molecular Physiology and Biophysics, Baylor College of Medicine, Houston, TX 77030, USA; [22]The Jan and Dan Duncan Neurological Research Institute, Houston, TX 77030, USA; [23]Department of Pediatrics, Baylor College of Medicine, Houston, TX 77030, USA; [24]Medical Research Council Harwell (Mammalian Genetics Unit and Mary Lyon Centre), Harwell, Oxfordshire OX11 0RD, UK; [25]Berlin Institute of Health, 10117 Berlin, Germany; [26]Dan L. Duncan Cancer Center, Baylor College of Medicine, Houston, TX 77030, USA
[27]These authors contributed equally to this work
[28]These authors contributed equally to this work
*Correspondence: heaney@bcm.edu (J.D.H.), mwalkiew@bcm.edu (M.A.W.)
http://dx.doi.org/10.1016/j.ajhg.2017.03.001.

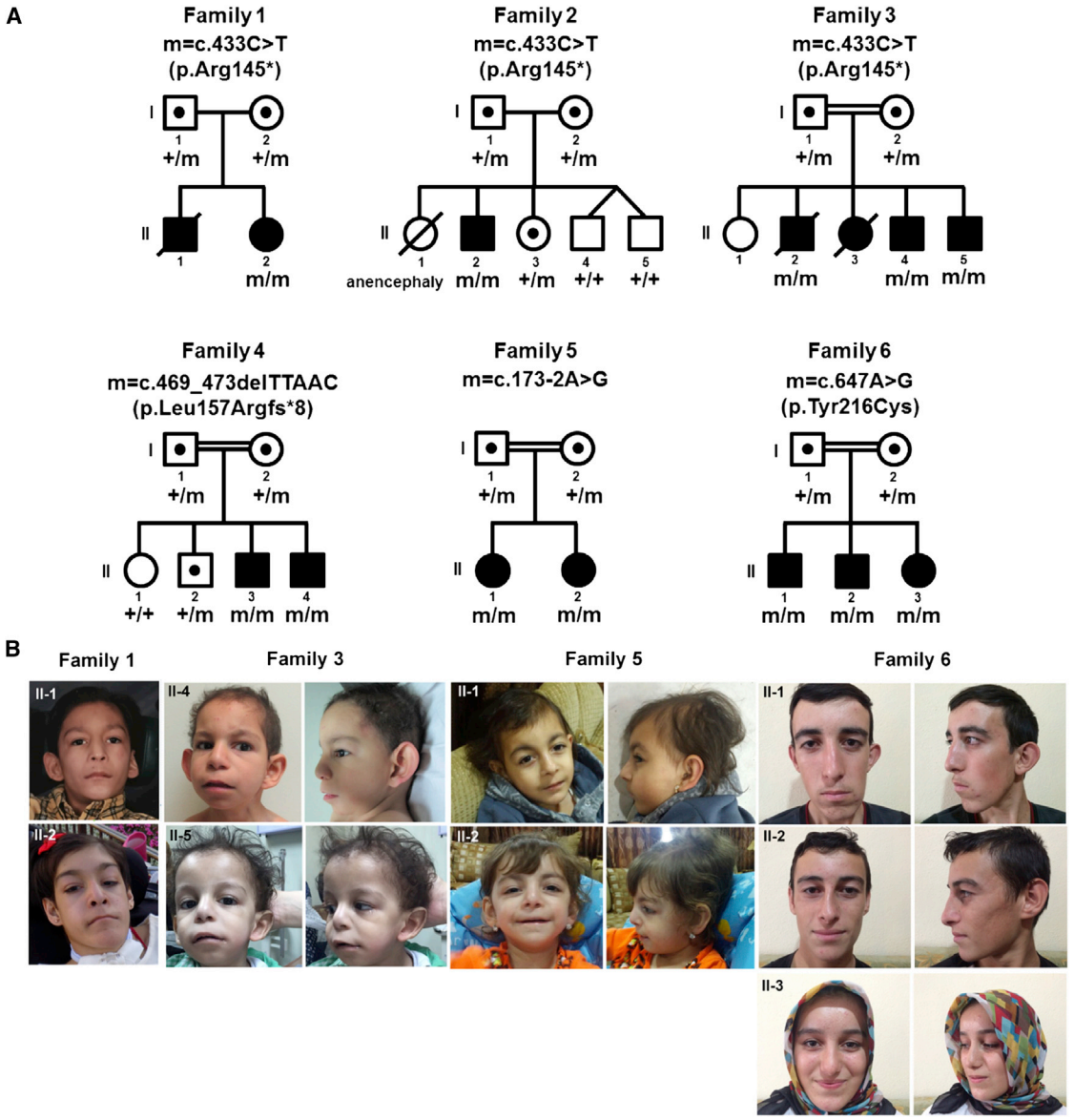

Figure 1. Pedigrees and Clinical Features of Families with Pathogenic Variants in *OTUD6B*
(A) Families with biallelic variants in *OTUD6B*. Allelic status is given below each tested individual. Symbols are as follows: filled, affected; empty, unaffected; dotted, heterozygous carrier; hash, deceased.
(B) Facial photos of affected individuals from families 1, 3, 5, and 6.

A summary of clinical findings is provided in Table 1, detailed case summaries can be found in the Supplemental Note, and pedigrees and photos are available in Figure 1. Of the six families with variants in *OTUD6B*, two were nonconsanguineous and four consanguineous. The cohort comprised eight males and four females, ages 3 to 20 years. All subjects exhibited intellectual disability. Nine subjects (75%) were severely impaired with absent speech and significant global developmental delay, and three subjects had only mild to moderate intellectual disability without delay in language or motor development. All subjects presented with seizures, mostly of the generalized tonic-clonic type, but with varying degrees of severity and frequency (from one episode to daily, refractory epilepsy). Other seizure types noted were absence, myoclonic, and atonic seizures. In nine subjects, particularly those with severe intellectual disability, additional recurrent features included severe microcephaly (Z-scores between −2.8 and −6.5), hypotonia, gross motor delay, and growth retardation. Intrauterine growth restriction (IUGR) was observed in seven pregnancies (58%). Nine subjects had feeding difficulties, which were evident as early as the neonatal period and required gastrostomy tube feeds for three subjects. Six subjects never walked independently. One subject (II-2 in family 1) with congenital spastic quadriplegia is able to walk short distances but is largely wheelchair dependent. One subject (II-2 in family 2) who did attain walking subsequently lost this ability due to severe and progressive spasticity. Among 12 subjects with neuroimaging studies, 6 showed structural brain abnormalities (50%) including

Table 1. Clinical Features of Subjects with Biallelic *OTUD6B* Variants

	Family 1	Family 2	Family 3			Family 4		Family 5		Family 6		
	II-2	II-2	II-2	II-4	II-5	II-3	II-4	II-1	II-2	II-1	II-2	II-3
Gender	female	male	male	male	male	male	male	female	female	male	male	female
Ethnic origin	Hispanic	Hispanic/Italy	Egypt	Egypt	Egypt	Syria	Syria	Palestine	Palestine	Turkey	Turkey	Turkey
Age at last examination	18 years, 2 months	17 years, 2 months	13 years (died same year)	8 years, 1 month	3 years	9 years, 5 months	3 years, 11 months	5 years, 4 months	3 years, 2 months	20 years, 7 months	16 years, 6 months	14 years, 8 months
Intellectual disability	severe	severe	severe	severe	severe	severe	severe	severe	severe	moderate	mild	moderate
Speech delay	no words	no words	no words	no words	no words	no words	no words	no words	no words	no delay	no delay	no delay
Seizure (onset)	+ (12 months)	+ (15 months)	+ (NA)	+ (NA)	+ (NA)	+ (17 months)	+ (3 years)	+ (7 months)	+ (2 years)	+ (18 months)	+ (7 years)	+ (8 years)
IUGR	+	+ (poor fetal activity)	+	+ (poor fetal activity)	+	+	+	−	−	−	−	−
Weight, kg (z-score)	28 (−8.9)	47.6 (−2.2)	15 (−2.2) (at 10 years)	12 (−4.5) (at 5 years)	9 (−3.5)	15.5 (−1.6) (at 5 years 2 months)	15 (−1)	15.6 (−1.4)	10 (−3.4)	67 (−0.33)	66 (0.27)	54 (0.27)
Height, cm (z-score)	129.5 (−5.2)	137 (−4.9)	103 (−5) (at 10 years)	90 (−3.8) (at 5 years)	80 (−3.7)	107 (−0.6) (at 5 years 2 months)	93 (−2.5)	100 (−2.1)	87 (−2.0)	176 (−0.1)	171 (−0.5)	159 (−0.4)
OFC, cm (z-score)	47.9 (−4.7)	52 (−2.8)	44.5 (−6.5) (at 10 years)	44 (−5.3) (at 5 years)	43 (−5.3)	46.5 (−3.5) (at 5 years 2 months)	45 (−4.3)	45 (−4.5)	44 (−4.3)	55.7 (−0.35)	54.5 (−0.59)	54.3 (0.38)
Hypotonia	+	+	+	+	+	+	+	+	+	−	−	−
Gross motor delay	congenital quadriplegic, mostly in wheelchair	walked at 3 years 9 months but now non-ambulatory	could sit, non-ambulatory	sits, non-ambulatory	does not sit, non-ambulatory	walked 4 years 6 months	sits, non-ambulatory	crawled at 3 years; stands and walks only with support	does not crawl or pull to stand, non-ambulatory	no delay	no delay	no delay
Feeding difficulties	+	+	+	+	+	+	+	+	+	−	−	−
Others	FTT, chronic constipation, G-tube feeds	FTT, chronic constipation and diarrhea, G-tube feeds	FTT	FTT	FTT	FTT	FTT, G-tube feeds					
Additional neurologic features	congenital quadriplegia, ataxia, spasticity	cerebral palsy, ataxia, spastic quadriplegia	autism spectrum disorder	autism spectrum disorder	autism spectrum disorder	−	−	−	−	−	−	−

(*Continued on next page*)

Table 1. ***Continued***

	Family 1	Family 2	Family 3			Family 4		Family 5		Family 6		
	II-2	**II-2**	**II-2**	**II-4**	**II-5**	**II-3**	**II-4**	**II-1**	**II-2**	**II-1**	**II-2**	**II-3**
Brain imaging	normal	prominent perivascular spaces, hypoplastic corpus callosum, generalized white matter volume loss, gliosis in bilateral parietal lobes	mild fronto-parietal cortical changes	mild fronto-parietal cortical changes, short corpus callosum	mild fronto-parietal cortical changes	normal	cortical and white matter atrophy	mild dilatation of lateral ventricles mainly occipital horns, deep interhemispheric fissure/ hypoplastic corpus callosum	normal	normal	normal	normal
Physical Features												
CHD	NA	normal echo	PS, ASD	normal echo	PS, ASD, VSD	NA	VSD	NA	TOF, ASD	NA	NA	NA
Other congenital malformations	sacral dimple	spina bifida occulta, cryptorchidism	–	cryptorchidism	–	cryptorchidism	sacral dimple cryptorchidism	–	–	–	–	–
Head/Neck	displaced posterior hair whorl	brachycephaly, sparse hair	short neck, sloping shoulders	short neck, sloping shoulders	short neck, sloping shoulders	–	–	flat occiput, sparse hair	flat occiput	wide forehead, narrow long asymmetric face	wide forehead, narrow long face	narrow long face
Eyes	arched eyebrows, long eyelashes, long palpebral fissures	arched eyebrows, long down-slanting palpebral fissures, ptosis	long palpebral fissures	long palpebral fissures	long palpebral fissures	long palpebral fissures	–	arched eyebrows, deep-set eyes, long eyelashes	deep-set eyes, long eyelashes	down-slanting palpebral fissures	–	–
Nose	long nose, hypoplastic alae, high nasal bridge, long philtrum	prominent nasal bridge, short columella, small alae, smooth long philtrum	broad root and prominent nasal bridge, smooth long philtrum	broad root and prominent nasal bridge, smooth long philtrum	broad root and prominent nasal bridge, smooth long philtrum	–	–	slightly long philtrum	slightly long philtrum	tubular nose	–	–
Mouth/Chin	high arched palate, cupid bow, dental crowding	thin upper lip, downturned mouth corners, high arched palate, mild retrognathia	very thin upper lip, retrognathia	very thin upper lip, retrognathia	very thin upper lip, retrognathia	–	–	thin upper lip	thin upper lip	high arched palate, dental malocclusion, narrow chin	high arched palate, narrow chin	high arched palate
Ears	–	posteriorly rotated ears, bilateral pits	large protruding low-set ears	large protruding low-set ears	large protruding low-set ears	large ears	large ears	large ears	large ears	prominent, dysplastic ears	–	–

(*Continued on next page*)

Table 1. *Continued*

	Family 1	Family 2	Family 3			Family 4		Family 5		Family 6		
	II-2	II-2	II-2	II-4	II-5	II-3	II-4	II-1	II-2	II-1	II-2	II-3
Scoliosis	+	+	+	–	–	–	+	+	–	–	–	–
Extremities	broad thumbs, tapered fingers, long first toes, joint contractures, brachydactyly of other toes, hallux valgus	broad thumbs, bulbous finger tips, forearm asymmetry, feet turned outward, joint contractures overriding toes, planovalgus	broad thumbs, clubbed fingers, clubfoot	broad thumbs, hyperextensibility of interphalangeal joints, overriding toes	broad thumbs, hyperextensibility of interphalangeal joints, overriding toes	broad thumbs and first toes, fetal pads	–	bilateral toe syndactyly	bilateral toe syndactyly	arachnodactyly	hyperextensibility of elbows	arachnodactyly, hyperextensibility of elbows

Abbreviations are as follows: IUGR, intrauterine growth restriction; OFC, occipitofrontal circumference; NA, not available; CHD, congenital heart disease; PS, pulmonic stenosis; VSD, ventricular septal defect; ASD, atrioseptal defect; TOF, tetralogy of Fallot; FTT, failure to thrive. For weight and height, data were obtained from last examination, unless otherwise noted. *Z*-scores were calculated using the CDC charts for children ages 2–20. For head circumference, *z*-score was calculated based on published data.[38]

cortical changes/white matter volume loss (n = 5), abnormal corpus callosum (n = 3), and dilatation of lateral ventricles (n = 1) (Figure S1).

Dysmorphic features were noted in all individuals. Shared facial features included large/protruding ears (n = 8), long philtrum (n = 7), thin upper lip (n = 6), long palpebral fissures (n = 6), high arched palate (n = 5), prominent/high nasal bridge (n = 5), retrognathia (n = 4), and arched eyebrows (n = 3). Abnormalities of fingers and/or toes were also common (n = 10), including broad thumbs (n = 6), overriding toes (n = 3), bulbous finger tips/fetal pads (n = 2), syndactyly (n = 2), arachnodactyly (n = 2), and brachydactyly (n = 1). Other shared features included progressive scoliosis (n = 5), hyperextensible joints (n = 4), joint contractures/clubfoot (n = 3), and sacral dimple/spina bifida occulta (n = 3). Four subjects had congenital heart defects including atrioseptal defect (n = 3), ventricular septal defect (n = 2), pulmonic stenosis (n = 2), and tetralogy of Fallot (n = 1). Four of eight males (50%) had either unilateral or bilateral cryptorchidism.

Not included in the study cohort are two additional deceased affected subjects (II-1 in family 1 and II-3 in family 3) for whom DNA samples were unavailable (Figure 1). Subject II-1 in family 1 had intellectual disability, intractable seizures, poor growth, sacral dimple, progressive scoliosis, and bilateral toe polydactyly. He died at age 12 years due to complications associated with Lennox-Gastaut syndrome. Subject II-3 in family 3 had a congenital heart defect, dysmorphic facial features, and delayed milestones. She died at age 2 years due to recurrent pulmonary infections. Based on the significant overlap of clinical features with those in our study cohort, we suspect that these individuals also carried biallelic pathogenic variants in *OTUD6B*.

A summary of molecular findings is provided in Figure 1 and Table 2. Four homozygous variants in *OTUD6B* (GeneBank: NM_016023.3; ClinVar: SCV000492514, SCV000492515, SCV000492516, SCV000492517)—one nonsense, one frameshift, one splice variant, and one missense variant—were identified by WES or whole-genome sequencing (family 6) and subsequently confirmed by Sanger sequencing. Consistent with a recessive mode of inheritance, the unaffected parents in all of the families were heterozygous for the respective familial variants, and all tested unaffected siblings (in families 2 and 4) were either heterozygous for the variant or homozygous for the reference allele. The available affected individuals in families 1, 2, and 3 shared the same homozygous nonsense variant, c.433C>T (p.Arg145*), located in exon 4 (Figure 2). This variant is annotated in dbSNP 147 (rs368313959) and has a maximum subpopulation allele frequency in the Latino population of 0.0026 (5/1,898 alleles) in the Exome Aggregation Consortium (ExAC) database and 0.00079 (25/31,718) in the Genome Aggregation Database (gnomAD) (Table 2). Therefore, this variant is significantly enriched in our cohort (6 of 12 alleles from 6 families versus 5 of 1,898 reference alleles from the Latino

Table 2. Variants in *OTUD6B*

	Families 1,2,3	Family 4	Family 5	Family 6
Genomic position (hg19)	8: 92,090,611	8: 92,090,647–92,090,651	8: 92,083,364	8: 92,090,825
Exon/Intron	exon 4	exon 4	intron 1	exon 4
Nucleotide change	c.433C>T	c.469_473delTTAAC	c.173−2A>G	c.647A>G
Protein change	p.Arg145*	p.Leu157Argfs*8	–	p.Tyr216Cys
Allele Frequency in ExAC				
Total	8/43,688 = 0.00018	not present	not present	not present
Latino	5/1,898 = 0.0026	–	–	–
African	1/4,386 = 0.000023	–	–	–
South Asian	2/8,864 = 0.000023	–	–	–
Number of homozygotes	none	–	–	–
Allele Frequency in gnomAD				
Total	32/239,902 = 0.00013	not present	not present	not present
Latino	25/31,718 = 0.00079	–	–	–
African	1/22,484 = 0.000044	–	–	–
South Asian	1/25,966 = 0.000039	–	–	–
Number of homozygotes	none	–	–	–
SIFT	–	–	–	deleterious
PolyPhen2	–	–	–	probably damaging

Variant nomenclature is based on GenBank: NM_016023.3. Abbreviations are as follows: ExAC, Exome Aggregation Consortium; gnomAD, Genome Aggregation Database.

population in ExAC, $p = 6.295 \times 10^{-12}$; Fisher's exact test). The calculated prevalence of individuals who are homozygous for this variant based on random mating would therefore be approximately 1/145,000 in the Latino population. This variant is not present in the homozygous state in ExAC or gnomAD, but this locus was covered in only 949 and 15,859 Latino individuals in these databases, respectively. Of note, families 1 and 2 were reported to be non-consanguineous, and both are of Hispanic descent. Illumina HumanExome-12v1 (cSNP) array data of the affected subjects from these families showed that *OTUD6B* lies in a small stretch of absence of heterozygosity (AOH) (5.4 Mb and 7.4 Mb, respectively) in chromosome 8. Also, AOH is seen in multiple chromosomes in these subjects, suggesting that AOH regions likely occurred through identity-by-descent. The affected subjects in families 4, 5, and 6 carried a homozygous frameshift variant (c.469_473delTTAAC [p.Leu157Argfs*8]), a homozygous splice variant (c.173−2A>G), and a homozygous missense variant (c.647A>G [p.Tyr216Cys]), respectively. These variants were not reported in ExAC or gnomAD.

OTUD6B maps to chromosome 8q21.3 and encodes a member of the ovarian tumor (OTU) domain-containing subfamily of deubiquitinating enzymes (DUBs). It consists of seven exons that encode a 323-amino acid protein (Figures 2A and 2B). The predicted protein contains several coiled coil (CC) domains and a conserved OTU domain, which is associated with cysteine protease activity. The predicted catalytic residues that function together at the center of the enzyme's active site are Asp185, Cys188, and His307; the C-loop, variable loop, and H-loop are the predicted ubiquitin-binding regions (Figures 2B and 2D). The location of the variants identified in our cohort in relation to the gene structure is shown in Figure 2. The truncating variants c.433C>T and c.469_473delTTAAC are predicted to lead to nonsense-mediated decay of the mRNA molecule. The c.173−2A>G variant affects an intronic splice acceptor site and is predicted to cause exon 2 skipping and introduction of a premature termination codon. This change is also predicted to result in nonsense-mediated decay of the mRNA molecule. The c.647A>G (p.Tyr216Cys) variant affects a highly evolutionarily conserved tyrosine residue in the OTU domain and is predicted to be deleterious by SIFT and PolyPhen-2 prediction tools (Figure 2C and Table 2). This tyrosine residue is also highly conserved among other OTU domain-containing enzymes and is located between the C-loop and variable loop (Figure 2D). Notably, subjects with predicted loss-of-function alleles (families 1 to 5) have a very severe clinical presentation while subjects with the missense variant (family 6) have a milder phenotype, suggestive of a hypomorphic allele (Table 1).

The International Mouse Phenotyping Consortium (IMPC) is generating a knockout mouse strain for every protein-coding gene in the mouse genome and is employing a standardized, broad-based adult and embryonic phenotyping of the knockout mice to identify gene-to-phenotype associations.[6,7] A C57BL/6N mouse

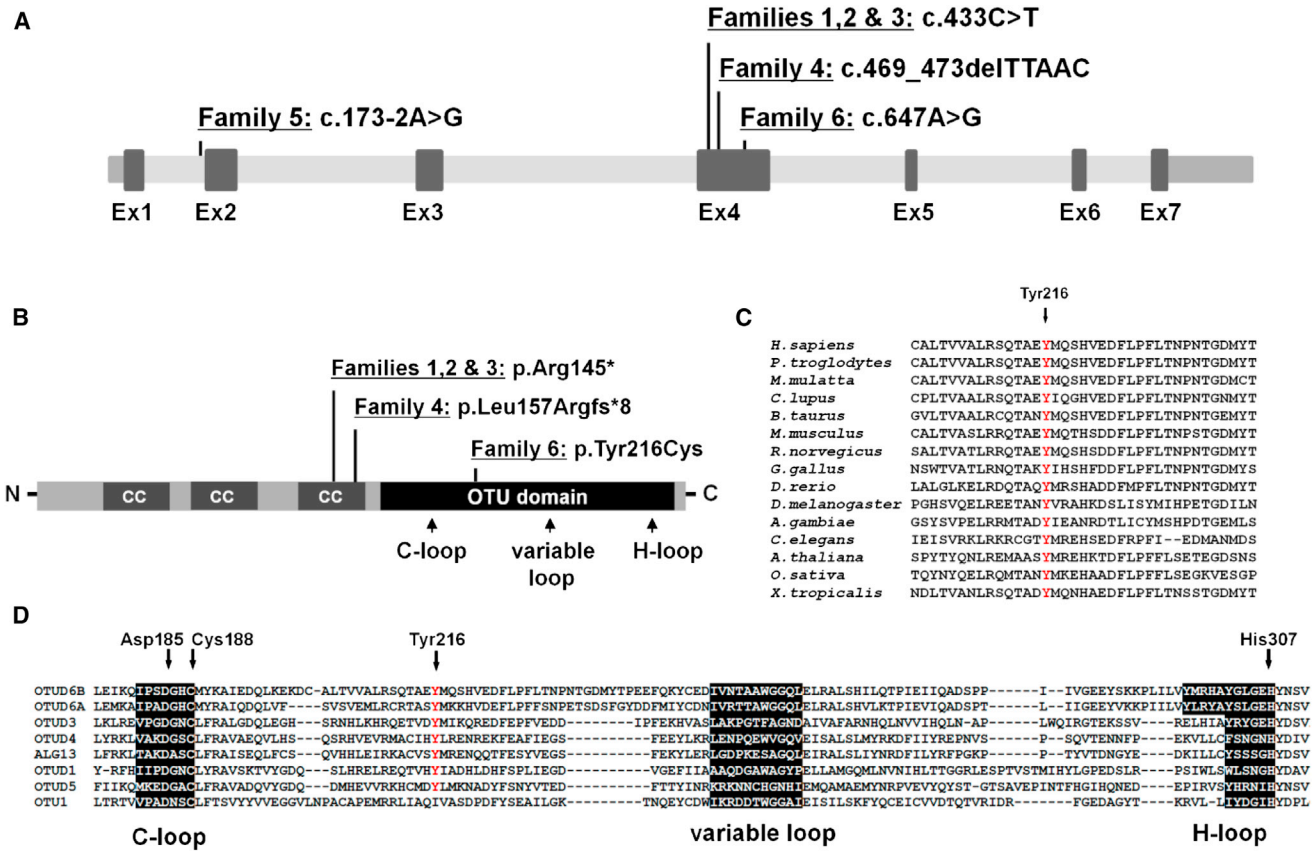

Figure 2. Location of Variants in *OTUD6B* and Conservation of the Substituted Tyrosine Residue in Orthologous and Paralogous Proteins

(A) Three of the *OTUD6B* variants in the described families are located in exon 4 of *OTUD6B* (GenBank: NM_016023.3, GRCH37/hg19). One is located in a canonical splice acceptor site in intron 1.

(B) Approximate location of amino acid changes relative to key functional domains of the OTUD6B protein (GenBank: NP_057107.3) including three coiled coil domains (CC) and an OTU-like cysteine protease domain. Also shown are the locations of the conserved predicted ubiquitin binding sites within the OTU domain: cysteine loop (C-loop), histidine loop (H-loop), and variable loop.

(C) Clustal Omega alignment of OTUD6B orthologs indicated the substituted tyrosine 216 residue is well conserved across species.

(D) Sequence of the catalytic center of human OTU domain-containing enzymes showing the location of the conserved catalytic residues (Asp185, Cys188, and His307) indicated that tyrosine 216 is also highly conserved across human OTUD enzymes.

strain harboring a β-galactosidase (lacZ)-tagged, knockout allele of *Otud6b*, created by deletion of exon 4 (*Otud6b*$^{tm1b(EUCOMM)Wtsi}$) (Figure 3A), has been produced and phenotyped by the IMPC. Mice homozygous for the *Otud6b* knockout allele (*Otud6b*$^{tm1b/tm1b}$) were sub-viable. Out of a total of 97 animals born from heterozygous knockout intercrosses, only 2 homozygous mice (1 male and 1 female) were identified by genotyping tissues collected 1 day after birth, which significantly deviates from the expected Mendelian frequency of 1 wild-type:2 heterozygotes:1 homozygote ($p < 1 \times 10^{-5}$; Table S1). Both homozygotes were found dead at the time of tissue collection, indicating that death occurred on the day of birth. Importantly, the IMPC and others have previously shown that genes causing lethality in mice are enriched for human genes associated with disease.[6,8,9] Thus, the sub-viability of homozygous mice appears consistent with the severity of *OTUD6B* loss-of-function variants in humans.

The IMPC performed embryo phenotyping[6] to determine when *Otud6b*$^{tm1b/tm1b}$ animals die during embryogenesis, the tissue distribution of lacZ reporter expression in fetal tissue, and the developmental defects that may contribute to sub-viability. *Otud6b*$^{tm1b/tm1b}$ embryos were observed at the expected Mendelian frequencies on embryonic day (E) E18.5 (7 homozygotes in a total of 29 embryos), indicating that *Otud6b*$^{tm1b/tm1b}$ mice die between E18.5 and shortly after birth. Expression of the lacZ reporter was nearly ubiquitous. As reported by the IMPC, lacZ expression was observed in several anatomical locations in *Otud6b*$^{tm1b/tm1b}$ and *Otud6b*$^{tm1b/+}$ embryos, including the footplate and handplate, oral cavity (mandibular and maxillary processes), liver, lung, somite, tail, ear, eye, brain (forebrain, midbrain, and hindbrain), and heart (Figures 3B–3E and S2A–S2D). Analysis of micro computed tomography (μCT) images indicated that the E18.5 *Otud6b*$^{tm1b/tm1b}$ embryos ($n = 2$) were smaller (34% reduced total volume, not significant) than wild-type littermates ($n = 2$) (Figure S3). Interestingly, 7 out of 12 human subjects in our study cohort with biallelic variants in *OTUD6B* had IUGR (Table 1). Additionally, seven human

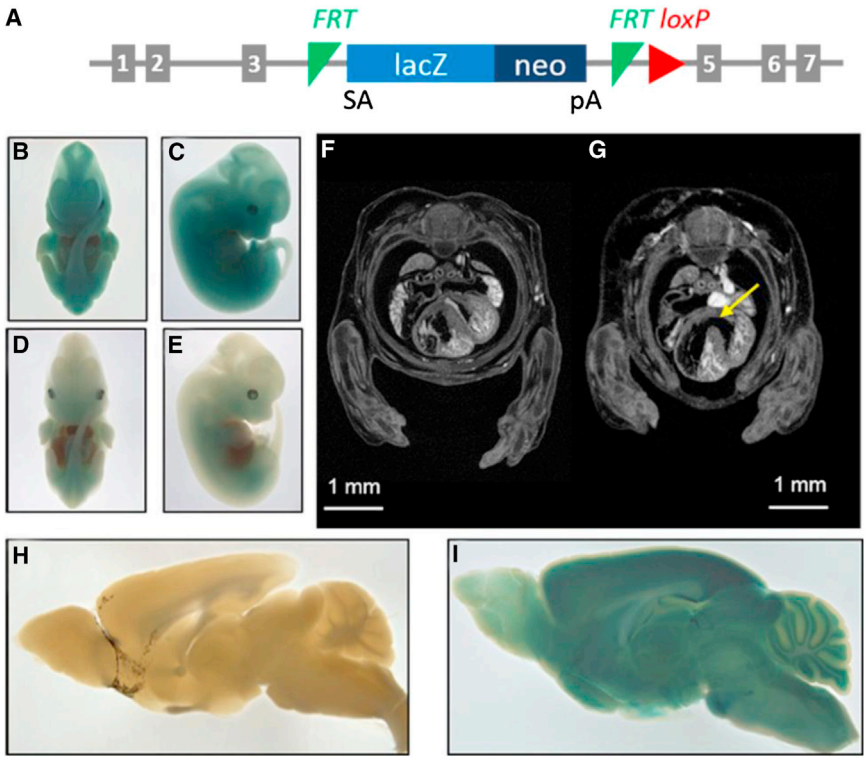

Figure 3. Phenotypic Effects of *Otud6b* Deficiency in Mice

(A) Schematic of the *Otud6b*^{tm1b} knockout allele. Exon 4 is deleted and β-galactosidase (lacZ) is expressed following splicing to exon 3 (SA = splice acceptor, pA = polyadenylation signal).

(B–E) LacZ expression, as determined by X-gal staining, from the *Otud6b*^{tm1b} allele is widespread in E12.5 *Otud6b*$^{tm1b/tm1b}$ (B, C) and *Otud6b*$^{tm1b/+}$ (D, E) embryos.

(F and G) Representative μCT image of E14.5 wild-type (F) and *Otud6b*$^{tm1b/tm1b}$ knockout (G) embryos. The ventricular septal defect in the *Otud6b*$^{tm1b/tm1b}$ knockout embryo is indicated (arrow).

(H and I) Representative X-gal staining images of wild-type (H) and *Otud6b*$^{tm1b/+}$ (I) adult brains (>50 days of age).

subjects had failure to thrive, and eight had small stature (Table 1). Furthermore, μCT imaging of *Otud6b*$^{tm1b/tm1b}$ embryos showed ventricular septal defects (VSDs) in 80% of hearts (3 of 3 E14.5 hearts with a VSD; 1 of 2 E18.5 hearts with a VSD) (Figures 3F, 3G, and S4). Blood obscured imaging of the heart in the E18.5 *Otud6b*$^{tm1b/tm1b}$ embryo in which a VSD could not be confirmed. Importantly, VSDs are not a common feature of the C57BL/6N inbred background. Only one VSD has been observed in 150 C57BL/6N embryos analyzed (0.67% incidence). Consistent with the high incidence of VSDs in *Otud6b*$^{tm1b/tm1b}$ mouse embryos, four human subjects in our study cohort had congenital heart defects, two of whom specifically had VSDs (Table 1).

Because homozygotes were sub-viable, heterozygous (*Otud6b*$^{tm1b/+}$) knockout male and female mice (n = 8 for each sex) were placed into the adult IMPC phenotyping pipeline, and values were compared to C57BL/6N controls. No significant differences in adult phenotypes were reported between *Otud6b*$^{tm1b/+}$ mice and wild-type controls (using the IMPC suggested p value of 1E-4). However, using the lacZ expression reporter in the *Otud6b* knockout allele, human disease-relevant expression patterns for *Otud6b* were identified in *Otud6b*$^{tm1b/+}$ adult mice. Expression of lacZ was observed in several organ systems including the cardiovascular system (heart and aorta), digestive system (large intestine and stomach), nervous system (spinal cord, peripheral nervous system, pituitary gland, and the brain), and musculoskeletal system (skeletal muscle and cartilage) (data not shown; available on the IMPC website). As reported by the IMPC, within the brain lacZ reporter expression was near ubiquitous, localizing to several anatomical locations including the olfactory bulb, cortex, cerebellum (granular and Purkinje layers with weak LacZ staining in the white matter), brain stem, hypothalamus, midbrain (inferior and superior colliculus), hippocampus (CA1/2/3 and subiculum), striatum, and thalamus (Figures 3H, 3I, and S2E). The widespread expression pattern of *Otud6b* in adult mice is consistent with a previous study showing *Otud6b* gene expression in multiple tissues.[10] Furthermore, it is consistent with the multiple organ systems affected in the described subjects, including the cardiovascular system (congenital heart defects), nervous system (cognitive disability, seizures, structural brain abnormalities, hypotonia, feeding and digestion issues), musculoskeletal system (scoliosis, abnormalities of the fingers/toes), and digestive system (feeding and digestion issues).

Post-translation modification by ubiquitin is an essential process that occurs in almost all cellular tissues in humans and other eukaryotes. Ubiquitin becomes covalently linked to target proteins by an isopeptide bond involving the ubiquitin C-terminal glycine and ε-amino group of a lysine within the target. Ubiquitination is mediated via the sequential action of a three enzyme conjugation pathway involving an E1-activating enzyme, an E2 conjugating enzyme, and an E3 ligase enzyme.[11,12] Ultimately, the attachment of ubiquitin, or chains of ubiquitin, to a protein substrate creates a signal for the protein's fate that is primarily associated with degradation via the 26S proteasome but may also result in changes in cellular location, protein activity, and interaction with other proteins.[13–15]

Ubiquitination is a reversible process countered by the action of DUBs, which are proteases that specifically cleave ubiquitin isopeptide linkages from protein substrates. Therefore, DUBs can regulate ubiquitin-dependent processes. The human genome encodes approximately 90

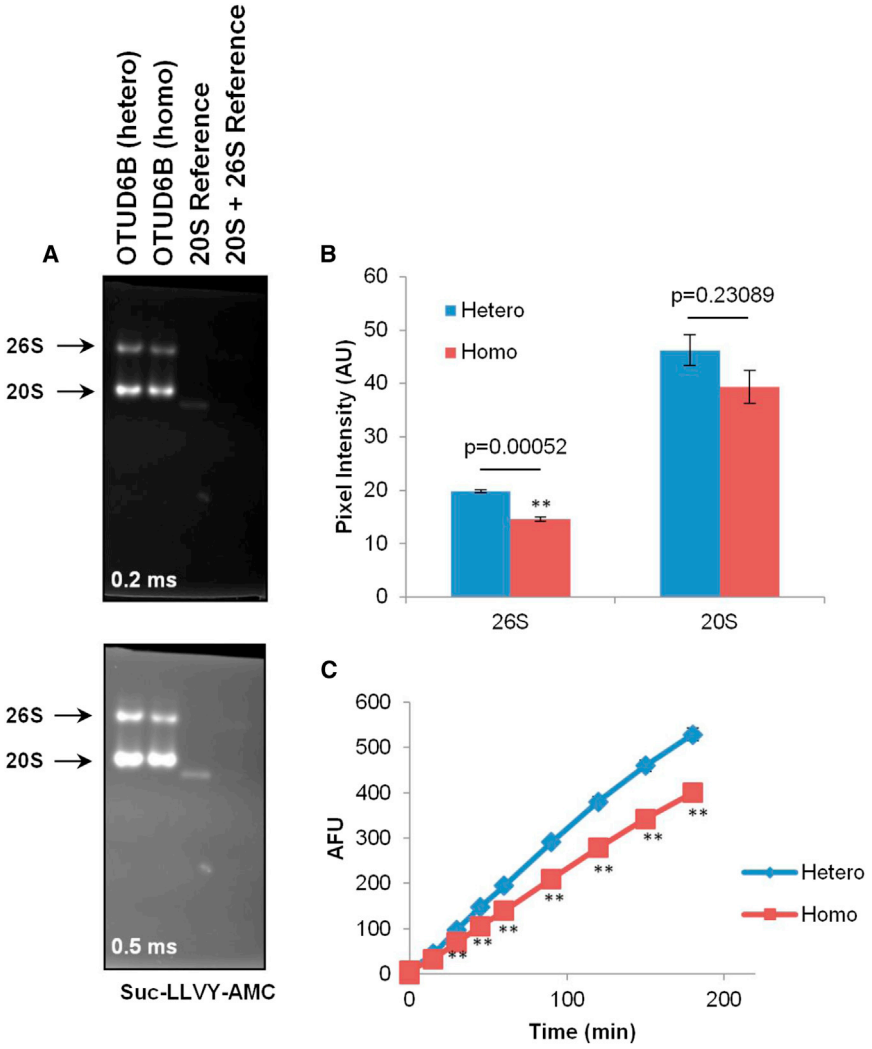

Figure 4. PBMCs from Individual Carrying the Homozygous c.469_473delTTAAC *OTUD6B* Deletion Exhibit Decreased Chymotrypsin-like Proteasome Activity

(A) Forty micrograms of whole-cell extracts of PBMCs derived from subjects with the heterozygous (hetero) or homozygous (homo) c.469_473delTTAAC *OTUD6B* deletion were separated by native PAGE, as indicated. Size controls in this experiment consisted of purified blood-derived 20S (20S reference) and a combination of 20S and 26S complexes (reference 20S + 26S) for 600 kDa and 1.2 MDa, respectively. Chymotrypsin-like proteasome activity was examined by incubating the gels with 0.1 mM of Suc-LLVY-AMC for 20 min at 37°C. Two exposure times (0.2 and 0.5 ms) at 360 nm are shown. One representative experiment of three is shown.

(B) Quantification of the 20S and 26S proteasome fluorescent bands from PBMCs with the hetero or homo c.469_473delTTAAC *OTUD6B* deletion by densitometry using the ImageJ 1.48v software. Shown is the mean pixel intensity calculated from three independent experiments following an exposure time of 0.3 ms. **$p < 0.001$ (Student's t test).

(C) Ten micrograms of whole-cell lysates from PBMCs carrying the hetero or homo *OTUD6B* deletion were incubated in quadruplicates with 0.1 mM Suc-LLVY in a final volume of 100 μL in non-denaturing conditions on 96-well plates. The fluorescence activity emerging from the release of AMC was measured at 360 nm every 15 min for the first hour, and then every 30 min for the last two hours. **$p < 0.01$ (Student's t test).

DUBs, which are classified into five subfamilies by their sequence diversity: ubiquitin C-terminal hydrolases (UCHs), ubiquitin-specific peptidases (USPs/UBPs), Josephin or Machado-Joseph disease (MJD) proteins, JAMM (Jab1/MPN domain-associated metalloisopeptidase) domain proteins, and lastly, the OTU-domain containing subfamily to which OTUD6B belongs. Several members of the OTU subfamily have been shown to regulate important signaling pathways including NF-κB signaling, interferon signaling, p97-mediated processes, and the DNA damage response.[16–21]

Given the potential role of OTUD6B in removing ubiquitin and/or ubiquitin chains from protein substrates, we reasoned that it may regulate the ubiquitin-proteasome system (UPS). To address the contribution of OTUD6B to the UPS, peripheral blood mononuclear cells (PBMCs) from subjects carrying a heterozygous or a homozygous c.469_473delTTAAC (p.Leu157Argfs*8) *OTUD6B* deletion (family 4; subjects I-1 and II-3, respectively) were analyzed for their proteasome content. To this end, proteasome complexes were separated on non-denaturing (native)-PAGE and visualized by their capacity to hydrolyze a Suc-LLVY-AMC fluorogenic substrate. As shown in Figure 4A, both of the 20S and 26S complexes from PBMCs of the homozygous subject exhibited weaker fluorescence intensity than those from the heterozygous subject, indicating that chymotrypsin-like activity was reduced in this sample. Densitometric analysis of the proteasome bands indicated that the intensity of the chymotrypsin-like activity of the 26S proteasome complexes from the homozygous subject was reduced by 20% when compared to those from the heterozygous subject (Figure 4B). Likewise, the activity of the 20S complexes in the homozygous sample was lower than that detected in the heterozygous sample, albeit not significantly. To further confirm these differences, the chymotrypsin-like activity was directly measured in whole-cell extracts by exposing them to 0.1 mM of the Suc-LLVY peptide for various periods of time. As shown in Figure 4C, the 26/20S complexes from the homozygous subject exhibited a decreased capacity to hydrolyze the Suc-LLVY substrate when compared to the same analysis on PBMCs from the heterozygous subject. This difference was statistically significant at all time points. This is in agreement with the data of our above-described, in-gel

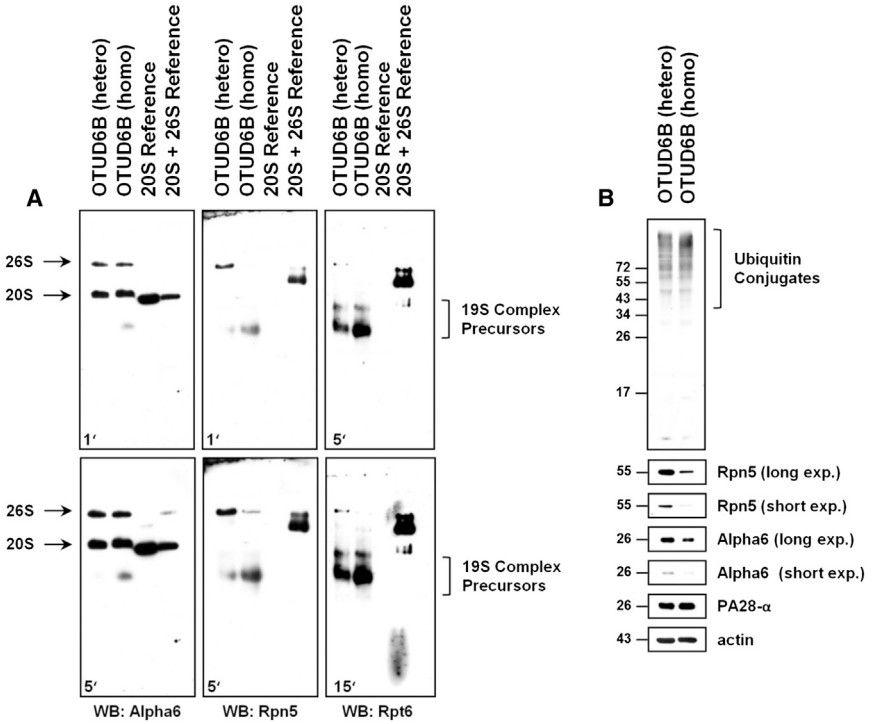

Figure 5. The Homozygous c.469_473delTTAAC *OTUD6B* Deletion Results in Decreased Amounts of 26S Proteasomes and Increased Accumulation of Ubiquitin-Protein Conjugates in PBMCs

(A) Forty micrograms of whole-cell extracts from PBMCs from subjects with the hetero or homo c.469_473delTTAAC *OTUD6B* deletion were resolved on native PAGE and subjected to western blotting using antibodies to Alpha6 (clone MCP20, Enzo Life Sciences), Rpn5 (clone H-9, Santa Cruz Biotechnology), and Rpt6 (clone p45-110, Enzo Life Sciences), as indicated. Controls consisted of 20S and 20S + 26S references, as described in Figure 4.

(B) Ten micrograms of protein lysates were separated by 15% SDS-PAGE followed by western blotting using antibodies specific for ubiquitin (ref #Z0458, DAKO GmbH), Rpn5 (clone H-9, Santa Cruz), Alpha6 (clone MCP20, Enzo Life Sciences), and PA28-α (K232/1, laboratory stock). Equal protein loading was ensured by probing the membranes with the anti-actin monoclonal antibody.

activity assays and therefore confirms that the homozygous c.469_473delTTAAC *OTUD6B* deletion compromises the chymotrypsin-like proteasome activity in PBMCs.

We next tested whether such impaired activity was due to a decreased amount of proteasome complexes in these samples. Protein-cell lysates derived from PBMCs from the heterozygous and homozygous subjects were resolved on native PAGE and subjected to western blotting to detect proteasome subunits: proteasome subunit alpha 6 (PSMA6 or Alpha6), proteasome 26S subunit, non-ATPase 12 (PSMD12 or Rpn5), and proteasome 26S subunit, ATPase 5 (PSMC5 or Rpt6). As illustrated in Figure 5A, probing the membrane with the Alpha6 antibody showed two strongly staining bands in both samples corresponding to the 20S and 26S proteasome complexes in these cells. Strikingly, the incorporation of the Rpn5 and Rpt6 subunits into 26S proteasomes was substantially reduced in the homozygous subject, as shown by decreased intensity of the Rpn5 and Rpt6 bands at the position of the 26S proteasome. These data strongly suggest that the c.469_473delTTAAC *OTUD6B* homozygous deletion is associated with a 26S proteasome assembly defect. In an attempt to determine whether the c.469_473delTTAAC *OTUD6B* deletion was a dominant or recessive genetic trait, the 26S proteasome populations from both of the heterozygous and homozygous *OTUD6B* subjects were then compared to those of *OTUD6B* wild-type individuals. To this end, proteasome complexes derived from PBMCs of four healthy blood donors were characterized using native-PAGE and western blotting, as described above. As expected, all four wild-type *OTUD6B* donors exhibit full incorporation of the Rpt6 and Rpn5 subunits in 26S proteasome complexes (Figure S5), confirming that the assembly pathway of the 19S regulatory particle was not compromised in these cells. To enable reliable comparison between wild-type, heterozygous, and homozygous *OTUD6B* subjects, our 26S reference was used as standard for normalization of the Rpn5 signal intensities emerging from cellular 26S proteasomes between experiments on different gels. Interestingly, our densitometric analysis showed that the relative amounts of Rpn5 in the 26S proteasome complexes was reduced by about 65% and 90% in the *OTUD6B* heterozygous and homozygous subjects, respectively, when compared with those of the *OTUD6B* wild-type controls (Figure S5), indicating that impaired proteasome assembly begins with the disruption of either of the two *OTUD6B* copies. This notion is fully in line with the observation that 19S precursor complexes accumulate in both of the heterozygous and homozygous subjects (Figure 5A) but not in wild-type controls (Figure S5). The lack of visible phenotype in the *OTUD6B* heterozygous subject suggests the existence of a compensation mechanism.

To further evaluate the functional significance of the c.469_473delTTAAC *OTUD6B* deletion, we next analyzed the cellular content of the ubiquitin-modified proteins in PBMCs in both of the heterozygous and homozygous subjects by SDS-PAGE. As shown in Figure 5B, the ubiquitin-protein conjugates accumulated much stronger in the homozygous sample than in the heterozygous one. This finding is in agreement with our previous observation that 26S proteasomes from the homozygous subject are defective. Interestingly, our SDS-PAGE analysis further confirmed a decrease in the total amount of the Rpn5

19S subunit and to a lesser extent of the Alpha6 subunit in PBMCs from the homozygous subject. By contrast, the steady-state expression level of the proteasome activator PA28-α remains unaffected in these cells. Interestingly, comparing both of the heterozygous and homozygous subjects with wild-type controls showed that the loss of one *OTUD6B* copy is sufficient to dramatically affect protein homeostasis, as evidenced by the accumulation of ubiquitin-protein conjugates in the *OTUD6B* heterozygous subject (Figure S6). Importantly, the increased amount of ubiquitin-modified proteins in subjects with the *OTUD6B* heterozygous and homozygous variant was paralleled by a substantial reduction of the steady-state expression level of the Rpt6 subunit in both of these samples (Figure S6). However, the expression level of the Rpn5 subunit was decreased in the homozygous *OTUD6B* subject but not in the heterozygous one, as determined by western blotting. Altogether, these data suggest that the c.469_473delTTAAC *OTUD6B* deletion results in proteasome malfunction whose severity proportionally increases with the number of affected alleles.

In this work, we identified the homozygous c.469_473delTTAAC *OTUD6B* deletion as a new member of the growing family of genetic alterations specifically affecting proteasome function.[22–26] To the best of our knowledge, the alteration described in this paper is the first one occurring outside the genes encoding the proteasome maturation protein (POMP) or any of seven alpha and/or beta proteasome subunits. The cellular loss-of-function phenotype of *OTUD6B* in the homozygous subject was characterized by a substantially reduced incorporation of 19S subunits into 26S proteasomes (Figure 5A) as well as decreased steady-state expression levels of 26S proteasome subunits (Figure 5B). Accordingly, this was accompanied by a drop of the chymotrypsin-like activity (Figure 4) and a concomitant accumulation of ubiquitin-protein conjugates (Figure 5B). It remains unclear whether the defect in 26S proteasome assembly detected in our native PAGE analysis is the cause or the consequence of the overall decreased expression of the proteasome subunits observed in SDS-PAGE. The accumulation of 19S precursor complexes in the homozygous subject suggests that the 19S subunits are not a rate-limiting factor for the formation of 26S proteasome complexes. It is therefore highly likely that the decreased steady-state levels of the proteasome subunits may reflect a higher susceptibility of these subunits to degradation due to their failure to incorporate into 26S proteasomes.

The precise mechanisms by which OTUD6B affects 26S proteasome assembly are ill defined and open unexpected avenues to understanding the regulation of protein homeostasis by the UPS. Given the described role of OTUD6B as a DUB, one can speculate that the formation of 26S complexes is a process regulated by ubiquitin modification. This notion would be in agreement with previous studies reporting the ubiquitination of various proteasome subunits including Rpn10, Rpn13, or Rpt5.[27–29] As such, it is conceivable that any impaired de-ubiquitination of these subunits might impact proteasome assembly and/or function. In this matter, further experiments will attempt to address the capacity of OTUD6B to remove ubiquitin from proteasome subunits.

Interestingly, by transmission electron microscopy, we identified abnormal cytoplasmic inclusions in lymphocytes from subject II-2 in family 2 (Figure S7). We speculate that these inclusions represent accumulation of protein substrates due to an imbalance in ubiquitination/deubiquitination activities in these cells. Although this study was performed in only one subject and only in lymphocytes, it raises the possibility that the inclusions might serve as a biomarker for this syndrome.

Many DUBs have been implicated in human diseases such as neurodegeneration, inflammation, infection, and cancer. For example, pathogenic variants in the ubiquitin-specific protease genes *USP9X* (MIM: 300072) and *USP27X* (MIM: 300975) cause X-linked intellectual disability (MIM: 300919, 300968, 300984). De novo loss-of-function variants in *USP7* (MIM: 602519) cause a neurodevelopmental disorder.[30] Trinucleotide repeat expansion in *ATXN3* (MIM: 607047) causes Machado-Joseph disease (MIM: 109150), a neurologic disorder characterized by ataxia, spasticity, and ocular movement abnormalities. Heterozygous truncating variants in *A20*/*TNFAIP3* (MIM: 191163) cause familial Behcet-like auto-inflammatory syndrome (MIM: 616744) and biallelic pathogenic variants in *OTULIN* (MIM: 615712) cause autoinflammation, panniculitis, and dermatosis syndrome (MIM: 617099). Germline variants in *BAP1* (MIM: 603089) and *CYLD* (MIM: 605018) can cause tumor predisposition syndromes (MIM: 614327, 132700). Maternal germline variants and de novo events in the human OTU domain-containing enzyme *ALG13* (MIM: 300776) cause early infantile epileptic encephalopathy 36 (MIM: 300884). Similarly, many ubiquitin ligase genes have been implicated in human diseases.[31–37] For example, defects in the *UBR1* (MIM: 605981), *MID1* (MIM: 300552), *MID2* (MIM: 300204), and *CUL4B* (MIM: 300304) have been associated with neurodevelopmental disorders.[31–34] Overall, this demonstrates the importance of the ubiquitination/deubiquitination process in human cells and that its disruption can lead to disease.

In summary, we describe a severe intellectual disability syndrome caused by biallelic loss-of-function variants in the deubiquitinating enzyme gene *OTUD6B*. This syndrome is characterized by cognitive dysfunction with absent speech, seizures, microcephaly, hypotonia, growth retardation, dysmorphism, and other variable features. We also describe a milder phenotype in humans with mild to moderate intellectual disability, seizures, and dysmorphic features caused by a homozygous missense variant in *OTUD6B* that is presumed to represent a hypomorphic allele. *Otud6b* knockout mice display several of the features seen in human subjects with *OTUD6B* loss-of-function variants and demonstrate the power of

the International Mouse Phenotyping Consortium as a resource for functional validation of novel disease genes. Finally, in vitro analyses implicate OTUD6B in proteasome function, thereby strengthening the notion that dysregulation of the ubiquitin system is causative of human disease.

Supplemental Data

Supplemental Data include Supplemental Note, seven figures, and one table and can be found with this article online at http://dx.doi.org/10.1016/j.ajhg.2017.03.001.

Consortia

The members of the Autosomal Recessive working group of the EuroEPINOMICS RES Consortium are Zaid Afawi, Rudi Balling, Nina Barisic, Stéphanie Baulac, Dana Craiu, Peter De Jonghe, Rosa Guerrero-Lopez, Renzo Guerrini, Ingo Helbig, Helle Hjalgrim, Johanna Jähn, Karl Martin Klein, Eric Leguern, Holger Lerche, Carla Marini, Hiltrud Muhle, Felix Rosenow, José Serratosa, Katalin Sterbová, Arvid Suls, Rikke S. Moller, Pasquale Striano, Yvonne Weber, and Federico Zara.

Acknowledgments

We thank the subjects and their families for participating in our research study. This work was supported by NIH K08DK106453 (L.C.B.), NIH U42OD011174 and NIH U54HG006348 (J.D.H., M.E.D., J.R.S., S. Wells, S.J.J., L.T.), NIH T32GM007526-39 (M.J.T.), the Trudy Mandel Louis Charitable Trust (O.E.), and the International Coordination Action grant G0E8614N (S. Weckhuysen, K.H.). The Eurocores program of the European Science Foundation supported the EuroEPINOMICS-RES network (G.A.136.11.N, FWO/ESF-ECRP, and HE5415/3-1). S.H. Caglayan is granted by the TUBITAK project no 110S518 within the Euroepinomics-RES network. The Family Genomics group at the Institute for Systems Biology deserves thanks for their support and project management of the whole-genome sequencing data (family 6). We acknowledge the contribution of Peter De Rijk (University of Antwerp) and the HPC facilities of the University of Luxembourg for computational support. The Department of Molecular and Human Genetics at the Baylor College of Medicine derives revenue from molecular genetic testing offered at the Baylor Miraca Genetics Laboratories. Since mid-October 2015, K.H. is under employment of UCB Pharma (Braine-l'Alleud, Belgium). The company had no part in this study.

Received: November 23, 2016
Accepted: February 21, 2017
Published: March 23, 2017

Web Resources

ClinVar, https://www.ncbi.nlm.nih.gov/clinvar/
Clustal Omega, http://www.ebi.ac.uk/Tools/msa/clustalo/
dbSNP, http://www.ncbi.nlm.nih.gov/projects/SNP/
ExAC Browser, http://exac.broadinstitute.org/
gnomAD Browser, http://gnomad.broadinstitute.org/
Growth Charts, http://www.cdc.gov/growthcharts/clinical_charts.htm
HPC, https://hpc.uni.lu/
International Mouse Phenotyping Consortium, http://www.mousephenotype.org/
OMIM, http://www.omim.org/
UniProt, http://www.uniprot.org/

References

1. Yang, Y., Muzny, D.M., Reid, J.G., Bainbridge, M.N., Willis, A., Ward, P.A., Braxton, A., Beuten, J., Xia, F., Niu, Z., et al. (2013). Clinical whole-exome sequencing for the diagnosis of mendelian disorders. N. Engl. J. Med. *369*, 1502–1511.
2. Yang, Y., Muzny, D.M., Xia, F., Niu, Z., Person, R., Ding, Y., Ward, P., Braxton, A., Wang, M., Buhay, C., et al. (2014). Molecular findings among patients referred for clinical whole-exome sequencing. JAMA *312*, 1870–1879.
3. Lee, H., Deignan, J.L., Dorrani, N., Strom, S.P., Kantarci, S., Quintero-Rivera, F., Das, K., Toy, T., Harry, B., Yourshaw, M., et al. (2014). Clinical exome sequencing for genetic identification of rare Mendelian disorders. JAMA *312*, 1880–1887.
4. Sawyer, S.L., Hartley, T., Dyment, D.A., Beaulieu, C.L., Schwartzentruber, J., Smith, A., Bedford, H.M., Bernard, G., Bernier, F.P., Brais, B., et al.; FORGE Canada Consortium; and Care4Rare Canada Consortium (2016). Utility of whole-exome sequencing for those near the end of the diagnostic odyssey: time to address gaps in care. Clin. Genet. *89*, 275–284.
5. Sobreira, N., Schiettecatte, F., Valle, D., and Hamosh, A. (2015). GeneMatcher: a matching tool for connecting investigators with an interest in the same gene. Hum. Mutat. *36*, 928–930.
6. Dickinson, M.E., Flenniken, A.M., Ji, X., Teboul, L., Wong, M.D., White, J.K., Meehan, T.F., Weninger, W.J., Westerberg, H., Adissu, H., et al.; International Mouse Phenotyping Consortium; Jackson Laboratory; Infrastructure Nationale PHENOMIN, Institut Clinique de la Souris (ICS); Charles River Laboratories; MRC Harwell; Toronto Centre for Phenogenomics; Wellcome Trust Sanger Institute; and RIKEN BioResource Center (2016). High-throughput discovery of novel developmental phenotypes. Nature *537*, 508–514.
7. Koscielny, G., Yaikhom, G., Iyer, V., Meehan, T.F., Morgan, H., Atienza-Herrero, J., Blake, A., Chen, C.K., Easty, R., Di Fenza, A., et al. (2014). The International Mouse Phenotyping Consortium Web Portal, a unified point of access for knockout mice and related phenotyping data. Nucleic Acids Res. *42*, D802–D809.
8. Georgi, B., Voight, B.F., and Bućan, M. (2013). From mouse to human: evolutionary genomics analysis of human orthologs of essential genes. PLoS Genet. *9*, e1003484.
9. Dickerson, J.E., Zhu, A., Robertson, D.L., and Hentges, K.E. (2011). Defining the role of essential genes in human disease. PLoS ONE *6*, e27368.
10. Xu, Z., Zheng, Y., Zhu, Y., Kong, X., and Hu, L. (2011). Evidence for OTUD-6B participation in B lymphocytes cell cycle after cytokine stimulation. PLoS ONE *6*, e14514.
11. Pickart, C.M. (2001). Mechanisms underlying ubiquitination. Annu. Rev. Biochem. *70*, 503–533.
12. Schulman, B.A., and Harper, J.W. (2009). Ubiquitin-like protein activation by E1 enzymes: the apex for downstream signalling pathways. Nat. Rev. Mol. Cell Biol. *10*, 319–331.
13. Glickman, M.H., and Ciechanover, A. (2002). The ubiquitin-proteasome proteolytic pathway: destruction for the sake of construction. Physiol. Rev. *82*, 373–428.

14. Mukhopadhyay, D., and Riezman, H. (2007). Proteasome-independent functions of ubiquitin in endocytosis and signaling. Science *315*, 201–205.
15. Schnell, J.D., and Hicke, L. (2003). Non-traditional functions of ubiquitin and ubiquitin-binding proteins. J. Biol. Chem. *278*, 35857–35860.
16. Ernst, R., Mueller, B., Ploegh, H.L., and Schlieker, C. (2009). The otubain YOD1 is a deubiquitinating enzyme that associates with p97 to facilitate protein dislocation from the ER. Mol. Cell *36*, 28–38.
17. Hu, H., Brittain, G.C., Chang, J.H., Puebla-Osorio, N., Jin, J., Zal, A., Xiao, Y., Cheng, X., Chang, M., Fu, Y.X., et al. (2013). OTUD7B controls non-canonical NF-κB activation through deubiquitination of TRAF3. Nature *494*, 371–374.
18. Hymowitz, S.G., and Wertz, I.E. (2010). A20: from ubiquitin editing to tumour suppression. Nat. Rev. Cancer *10*, 332–341.
19. Kayagaki, N., Phung, Q., Chan, S., Chaudhari, R., Quan, C., O'Rourke, K.M., Eby, M., Pietras, E., Cheng, G., Bazan, J.F., et al. (2007). DUBA: a deubiquitinase that regulates type I interferon production. Science *318*, 1628–1632.
20. Keusekotten, K., Elliott, P.R., Glockner, L., Fiil, B.K., Damgaard, R.B., Kulathu, Y., Wauer, T., Hospenthal, M.K., Gyrd-Hansen, M., Krappmann, D., et al. (2013). OTULIN antagonizes LUBAC signaling by specifically hydrolyzing Met1-linked polyubiquitin. Cell *153*, 1312–1326.
21. Nakada, S., Tai, I., Panier, S., Al-Hakim, A., Iemura, S., Juang, Y.C., O'Donnell, L., Kumakubo, A., Munro, M., Sicheri, F., et al. (2010). Non-canonical inhibition of DNA damage-dependent ubiquitination by OTUB1. Nature *466*, 941–946.
22. Brehm, A., Liu, Y., Sheikh, A., Marrero, B., Omoyinmi, E., Zhou, Q., Montealegre, G., Biancotto, A., Reinhardt, A., Almeida de Jesus, A., et al. (2015). Additive loss-of-function proteasome subunit mutations in CANDLE/PRAAS patients promote type I IFN production. J. Clin. Invest. *125*, 4196–4211.
23. Brehm, A., and Krüger, E. (2015). Dysfunction in protein clearance by the proteasome: impact on autoinflammatory diseases. Semin. Immunopathol. *37*, 323–333.
24. Kitamura, A., Maekawa, Y., Uehara, H., Izumi, K., Kawachi, I., Nishizawa, M., Toyoshima, Y., Takahashi, H., Standley, D.M., Tanaka, K., et al. (2011). A mutation in the immunoproteasome subunit PSMB8 causes autoinflammation and lipodystrophy in humans. J. Clin. Invest. *121*, 4150–4160.
25. Arima, K., Kinoshita, A., Mishima, H., Kanazawa, N., Kaneko, T., Mizushima, T., Ichinose, K., Nakamura, H., Tsujino, A., Kawakami, A., et al. (2011). Proteasome assembly defect due to a proteasome subunit beta type 8 (PSMB8) mutation causes the autoinflammatory disorder, Nakajo-Nishimura syndrome. Proc. Natl. Acad. Sci. USA *108*, 14914–14919.
26. Kunimoto, K., Kimura, A., Uede, K., Okuda, M., Aoyagi, N., Furukawa, F., and Kanazawa, N. (2013). A new infant case of Nakajo-Nishimura syndrome with a genetic mutation in the immunoproteasome subunit: an overlapping entity with JMP and CANDLE syndrome related to PSMB8 mutations. Dermatology (Basel) *227*, 26–30.
27. Isasa, M., Katz, E.J., Kim, W., Yugo, V., González, S., Kirkpatrick, D.S., Thomson, T.M., Finley, D., Gygi, S.P., and Crosas, B. (2010). Monoubiquitination of RPN10 regulates substrate recruitment to the proteasome. Mol. Cell *38*, 733–745.
28. Jacobson, A.D., MacFadden, A., Wu, Z., Peng, J., and Liu, C.W. (2014). Autoregulation of the 26S proteasome by in situ ubiquitination. Mol. Biol. Cell *25*, 1824–1835.
29. Cohen-Kaplan, V., Livneh, I., Avni, N., Fabre, B., Ziv, T., Kwon, Y.T., and Ciechanover, A. (2016). p62- and ubiquitin-dependent stress-induced autophagy of the mammalian 26S proteasome. Proc. Natl. Acad. Sci. USA *113*, E7490–E7499.
30. Hao, Y.H., Fountain, M.D., Jr., Fon Tacer, K., Xia, F., Bi, W., Kang, S.H., Patel, A., Rosenfeld, J.A., Le Caignec, C., Isidor, B., et al. (2015). USP7 acts as a molecular rheostat to promote WASH-dependent endosomal protein recycling and is mutated in a human neurodevelopmental disorder. Mol. Cell *59*, 956–969.
31. Geetha, T.S., Michealraj, K.A., Kabra, M., Kaur, G., Juyal, R.C., and Thelma, B.K. (2014). Targeted deep resequencing identifies MID2 mutation for X-linked intellectual disability with varied disease severity in a large kindred from India. Hum. Mutat. *35*, 41–44.
32. Quaderi, N.A., Schweiger, S., Gaudenz, K., Franco, B., Rugarli, E.I., Berger, W., Feldman, G.J., Volta, M., Andolfi, G., Gilgenkrantz, S., et al. (1997). Opitz G/BBB syndrome, a defect of midline development, is due to mutations in a new RING finger gene on Xp22. Nat. Genet. *17*, 285–291.
33. Zenker, M., Mayerle, J., Lerch, M.M., Tagariello, A., Zerres, K., Durie, P.R., Beier, M., Hülskamp, G., Guzman, C., Rehder, H., et al. (2005). Deficiency of UBR1, a ubiquitin ligase of the N-end rule pathway, causes pancreatic dysfunction, malformations and mental retardation (Johanson-Blizzard syndrome). Nat. Genet. *37*, 1345–1350.
34. Zou, Y., Liu, Q., Chen, B., Zhang, X., Guo, C., Zhou, H., Li, J., Gao, G., Guo, Y., Yan, C., et al. (2007). Mutation in CUL4B, which encodes a member of cullin-RING ubiquitin ligase complex, causes X-linked mental retardation. Am. J. Hum. Genet. *80*, 561–566.
35. Kishino, T., Lalande, M., and Wagstaff, J. (1997). UBE3A/E6-AP mutations cause Angelman syndrome. Nat. Genet. *15*, 70–73.
36. Tomaić, V., and Banks, L. (2015). Angelman syndrome-associated ubiquitin ligase UBE3A/E6AP mutants interfere with the proteolytic activity of the proteasome. Cell Death Dis. *6*, e1625.
37. Kitada, T., Asakawa, S., Hattori, N., Matsumine, H., Yamamura, Y., Minoshima, S., Yokochi, M., Mizuno, Y., and Shimizu, N. (1998). Mutations in the parkin gene cause autosomal recessive juvenile parkinsonism. Nature *392*, 605–608.
38. Rollins, J.D., Collins, J.S., and Holden, K.R. (2010). United States head circumference growth reference charts: birth to 21 years. J. Pediatr. *156*, 907–913, 913.e1–913.e2.

The American Journal of Human Genetics, Volume *100*

Supplemental Data

Biallelic Variants in *OTUD6B* Cause an Intellectual Disability Syndrome Associated with Seizures and Dysmorphic Features

Teresa Santiago-Sim, Lindsay C. Burrage, Frédéric Ebstein, Mari J. Tokita, Marcus Miller, Weimin Bi, Alicia A. Braxton, Jill A. Rosenfeld, Maher Shahrour, Andrea Lehmann, Benjamin Cogné, Sébastien Küry, Thomas Besnard, Bertrand Isidor, Stéphane Bézieau, Isabelle Hazart, Honey Nagakura, LaDonna L. Immken, Rebecca O. Littlejohn, Elizabeth Roeder, EuroEPINOMICS RES Consortium Autosomal Recessive working group, S. Hande Caglayan, Bulent Kara, Katia Hardies, Sarah Weckhuysen, Patrick May, Johannes R. Lemke, Orly Elpeleg, Bassam Abu-Libdeh, Kiely N. James, Jennifer L. Silhavy, Mahmoud Y. Issa, Maha S. Zaki, Joseph G. Gleeson, John R. Seavitt, Mary E. Dickinson, M. Cecilia Ljungberg, Sara Wells, Sara J. Johnson, Lydia Teboul, Christine M. Eng, Yaping Yang, Peter-Michael Kloetzel, Jason D. Heaney, and Magdalena A. Walkiewicz

Supplemental Data

Detailed clinical summaries

Family 1

Subject II-2 from Family 1 is an 18 year old female who was born to non-consanguineous Hispanic parents at 37 weeks gestational age by caesarean section (C-section) following a pregnancy complicated by intrauterine growth restriction (IUGR). She had congenital quadriplegia, jaundice, and feeding difficulties postnatally necessitating a 10 day admission to the neonatal intensive care unit (NICU). A sacral dimple and dysmorphic features were noted at that time. Her subsequent development was delayed. She sat independently at 9 months, walked at 18 months, and has not acquired language skills to date. She had onset of seizures at 1 year of age and was ultimately diagnosed with Lennox-Gastaut refractory epilepsy. At her most recent follow-up visit at 18 years of age, she had significant feeding problems including dysphagia and gastroesophageal reflux disease (GERD) that had required a Nissen procedure and gastrostomy-tube (G-tube) feeds and resulted in failure to thrive. Medical concerns included refractory seizures, respiratory insufficiency secondary to scoliosis requiring tracheostomy, recurrent infections, anemia, irregular menses, hypothyroidism, and bilateral hearing loss. On exam, she was noted to be nonverbal, minimally ambulatory, and had severe intellectual disability. Height was -5.2SD, weight was -8.9SD, and occipitofrontal circumference (OFC) was -4.7SD, consistent with global growth failure and microcephaly. She had long eyelashes, arched brows, long palpebral fissures, a displaced posterior hair whorl, a long nose, hypoplastic alae, high nasal bridge, long philtrum, high-arched palate, cupid bow, and dental crowding. Additional physical exam findings included abnormal tone and ataxia with abnormal posturing, severe kyphoscoliosis, multiple joint contractures, tapered fingers, long great toes with hallux valgus, brachydactyly of the 2^{nd} – 4^{th} toes, varus of the 5^{th} toe, and

high arches. Family history was notable for unaffected healthy parents and a similarly affected brother who died at age 12 years due to complications associated with Lennox-Gastaut syndrome.

Whole exome sequencing detected a homozygous c.433C>T (p.Arg145Ter) variant in *OTUD6B* in subject II-2. This variant was found as a heterozygous change in both parents. A sample was not available for testing of the deceased brother.

Family 2

Subject II-2 from Family 2 is a 17 year old male who was born to non-consanguineous parents of Hispanic and Italian descent at 36 weeks by spontaneous vaginal delivery following a pregnancy complicated by IUGR, poor fetal activity, and oligohydramnios. Postnatal concerns included irritability, feeding difficulties, lack of a rooting reflex, a high pitched cry, hypotonia of the arms with hypertonia of the legs, and presence of spina bifida occulta. Subsequent development was delayed. He sat independently at 18 months, walked independently at 3 years 9 months, and has acquired no language skills to date. He had onset of seizures at 15 months, including tonic-clonic seizures and staring spells. Athetoid movements were also noted in early childhood. At his most recent evaluation at 17 years of age, he had significant persistent feeding difficulties and GERD causing failure to thrive and requiring G-tube feeds. He had a vagal nerve stimulator for refractory epilepsy. He was partially ventilator dependent and had a history of obstructive sleep apnea, asthma, renal tubular acidosis, bilateral retractile testes, neurogenic bladder, sensorineural hearing loss, and growth hormone deficiency. Recurrent infections had prompted a diagnosis of hypogammaglobulinemia. On physical exam, he was nonverbal, non-ambulatory, and severely intellectually disabled. Height was -4.9SD, weight was -2.2SD, and OFC was -2.8SD, consistent with growth failure and microcephaly. On physical exam he had athetosis and abnormal tone including both hyper- and hypotonia. He was brachycephalic, had sparse scalp hair, full and arched brows, long and down-slanting palpebral fissures, mild ptosis, infraorbital

creases, posteriorly rotated ears with bilateral pits, a long nose with a convex nasal ridge, long smooth philtrum, high arched palate, thin upper lip, and mild retrognathia. Severe scoliosis was noted, as were joint contractures, broad thumbs, bulbous fingertips, and overlapping toes. Family history was notable for asymptomatic parents and three healthy siblings; one additional sister was reported to have died shortly after birth from anencephaly.

MRI of the brain demonstrated leukodystrophy, prominent Virchow-Robin spaces, hypoplastic corpus callosum, generalized white matter volume loss, gliosis in the bilateral parietal lobes, and mega cisterna magna. Whole exome sequencing performed on subject II-2 detected a homozygous c.433C>T (p.Arg145Ter) variant in *OTUD6B*. This variant was found as a heterozygous change in both parents and one healthy sibling. The other two healthy siblings were homozygous for the reference allele.

Family 3

Subject II-2 from Family 3 was a 13 year old male who was born to consanguineous parents of Egyptian descent by C-section at term following a pregnancy complicated by IUGR. Postnatally, he had a poor cry, weak movement, and feeding difficulties. He was diagnosed with congenital heart anomalies including pulmonic stenosis and an atrioseptal defect. His subsequent development was severely delayed. He learned to sit independently but not walk. He was seen for follow-up at age 10 years, at which time his height was -5SD, weight was -2.2SD, and OFC was -6.5SD, consistent with growth failure and microcephaly. At his most recent follow-up at 13 years of age, he carried a diagnosis of autism and of epilepsy with generalized tonic-clonic seizures. He had a history of persistent feeding difficulties. On exam, he was non-ambulatory, nonverbal, and severely intellectual impaired. Notable features included long palpebral fissures, large protruding and low set ears, a broad nasal root and prominent nasal bridge, long flat philtrum, thin upper lip, retrognathia, short neck, and sloping shoulders. He also had hypotonia, scoliosis, clubfoot, broad thumbs, and clubbed fingers. Subject II-2 died at 13 years of age

from recurrent pulmonary infections. Family history was significant for three affected siblings, including one sister (subject II-3) who died at 2 years of age also from recurrent pulmonary infections secondary to failure to thrive, and two brothers ages 8 years (subject II-4) and 3 years (subject II-5) at last follow-up. Both subjects II-4 and II-5 shared a strikingly similar phenotype with subject II-1, although subject II-4 did not have a known congenital heart defect, and both subjects II-4 and II-5 had the additional findings of hyperextensible interphalangeal joints and overriding toes.

Brain imaging demonstrated mild frontoparietal cortical changes in subject II-2 that were also seen in subjects II-4 and II-5. Whole exome sequencing detected a c.433C>T (p.Arg145Ter) variant in *OTUD6B* that was found to be homozygous in all three affected brothers and heterozygous in both parents. A sample was not available for testing of the deceased younger sister or the healthy older sister.

Family 4

Subject II-3 from Family 4 is a 9 year old boy born at 36 weeks by spontaneous vaginal delivery to consanguineous parents of Syrian ancestry following a pregnancy complicated by IUGR. He had onset of seizures at 17 months of age, and also had early developmental delay with independent ambulation achieved at 4.5 years of age. Subject II-3 was seen for follow-up at age 5 years, at which time his height was -0.6SD, weight was -1.6SD, and OFC was -3.5SD, consistent with microcephaly. At his most recent visit at age 9 years, he was nonverbal and had severe intellectual disability. He had a diagnosis of retinopathy with an abnormal electroretinogram (ERG). He had feeding difficulties causing failure to thrive. Notable features included hypotonia, long palpebral fissures, large ears, broad thumbs and first toes, and persistent fetal pads. Family history was remarkable for a similarly affected younger brother (subject II-4), also born by spontaneous vaginal delivery at 38 weeks gestational age. Subject II-4 had hypotonia and feeding difficulties in the neonatal setting requiring G-tube placement. He also had an interventricular septal defect, bilateral cryptorchidism, and sacral dimple. His motor and speech

development were delayed and he had one episode of seizure at 3 years of age. At his most recent follow-up visit at 3 years and 11 months, he had a diagnosis of hypothyroidism. On exam, he was nonverbal and non-ambulatory with severe intellectual disability. Height was -2.5SD, weight was -1SD, and OFC was -4.3SD consistent with short stature and microcephaly. He had large ears, was hypotonic, and had scoliosis.

Brain imaging performed on subject II-3 was normal while subject II-4 had cortical and white matter atrophy. Whole exome sequencing detected a homozygous c.469_473del (p.Leu157Argfs*8) variant in *OTUD6B* in both affected brothers. This variant was found as a heterozygous change in both parents and in one healthy sibling. The other healthy sibling is homozygous for the reference allele.

Family 5

Subject II-1 from Family 5 is a 5 year old female who was born to consanguineous Palestinian parents by spontaneous vaginal delivery at 38 weeks following an unremarkable pregnancy. There were no neonatal concerns however her development was subsequently delayed. She learned to sit independently at 24 months and crawl at 3 years. She had onset of myoclonic seizures at 7 months of age. At her most recent follow-up at 5 years of age, she could stand and walk with assistance, recognize her parents, was socially engaging, and was babbling. Height was -2.1SD, weight was -1.4SD, and OFC was -4.5SD. On exam, she had generalized hypotonia and was noted to have myoclonic movements. Notable features included sparse hair, a flat occiput, arched eyebrows, deep set eyes, long eyelashes, large ears, long philtrum, thin upper lip, scoliosis, and syndactyly of the 2nd and 3rd toes bilaterally. Family history was remarkable for unaffected parents and a similarly affected 3 year old younger sister (subject II-2) with significant phenotypic overlap. Subject II-2, however, had a history of more severe developmental delay and the additional finding of complex congenital heart disease including tetralogy of Fallot and a small atrioseptal defect.

Brain imaging performed on subject II-1 showed mild dilatation of the lateral ventricles, a deep interhemispheric fissure with hypoplasia of the corpus callosum, whereas brain CT performed on subject II-2 was normal. Whole exome sequencing detected a c.173-2A>G variant in *OTUD6B* that was found as a homozygous change in both affected siblings and as a heterozygous change in both parents.

Family 6

Subject II-1 from Family 6 is a 20 year old male who was born to consanguineous Caucasian parents at full term by normal spontaneous vaginal delivery. There were no neonatal complications and no early developmental delays. He had seizure onset at 18 months, with generalized tonic-clonic seizures occurring initially in the context of fever and subsequently during sleep, often with clustering. Learning problems emerged in primary school, and the subject learned to read and write but did not progress past 8th grade. At his most recent follow-up visit at 20 years of age, he had moderate intellectual disability. Height was at the 45th centile, weight at the 37th centile, and OFC at the 25th centile, consistent with normal stature and head circumference. He had a long narrow face with facial asymmetry, broad forehead, down-slanting palpebral fissures, prominent dysplastic and anteriorly angled ears, a tubular nose, high arched palate, occlusion anomalies of the teeth, a narrow chin, and arachnodactyly. Family history was remarkable for asymptomatic parents and two similarly affected siblings including a 16 year old brother (subject II-2) and a 14 year old sister (subject II-3). Both subjects II-2 and II-3 from family 6 were noted to have hyperextensibility of the elbow, which was not seen in the eldest brother.

Brain imaging studies performed on subjects II-1, II-2, and II-3 were normal. Whole-genome sequencing detected a c.647A>G (p.Tyr216Cys) variant in *OTUD6B* that was found as a homozygous change in all affected siblings and as a heterozygous change in both parents.

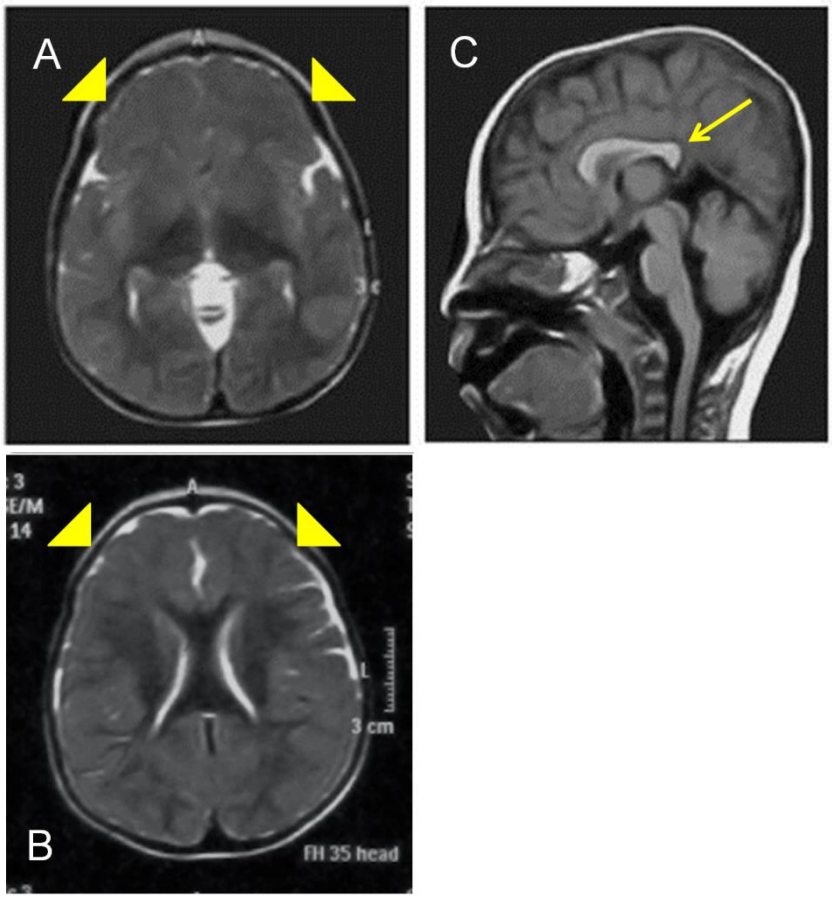

Figure S1. Brain structural abnormalities in Subject II-4 from Family 3.

Brain MRI images at age 1 year 11 months. Arrowheads indicate mild frontoparietal cortical changes **(A & B)** and the arrow indicates short corpus callosum **(C)**.

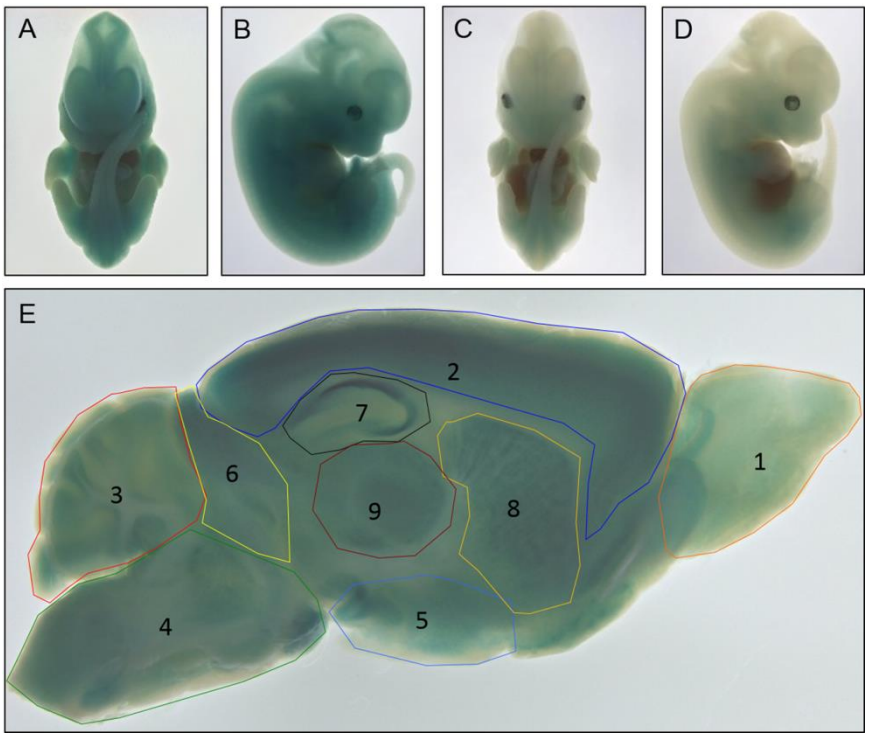

Figure S2. Otud6b expression in the mouse embryo and adult brain. (A-D) LacZ expression, as determined by X-gal staining, from the *Otud6b*^{tm1b} allele is widespread in E12.5 *Otud6b*$^{tm1b/tm1b}$ (A & B) and *Otud6b*$^{tm1b/+}$ (C & D) embryos. Enlarged images of the same embryos in Figure 3 B-E. **(E)** A representative X-gal staining image of an *Otud6b*$^{tm1b/+}$ adult brain (> 50 days of age). Expression of the lacZ reporter localized to several anatomical locations including (1) olfactory bulb, (2) cortex, (3) cerebellum, (4) brain stem, (5) hypothalamus, (6) midbrain, (7) hippocampus, (8) striatum, and (9) thalamus.

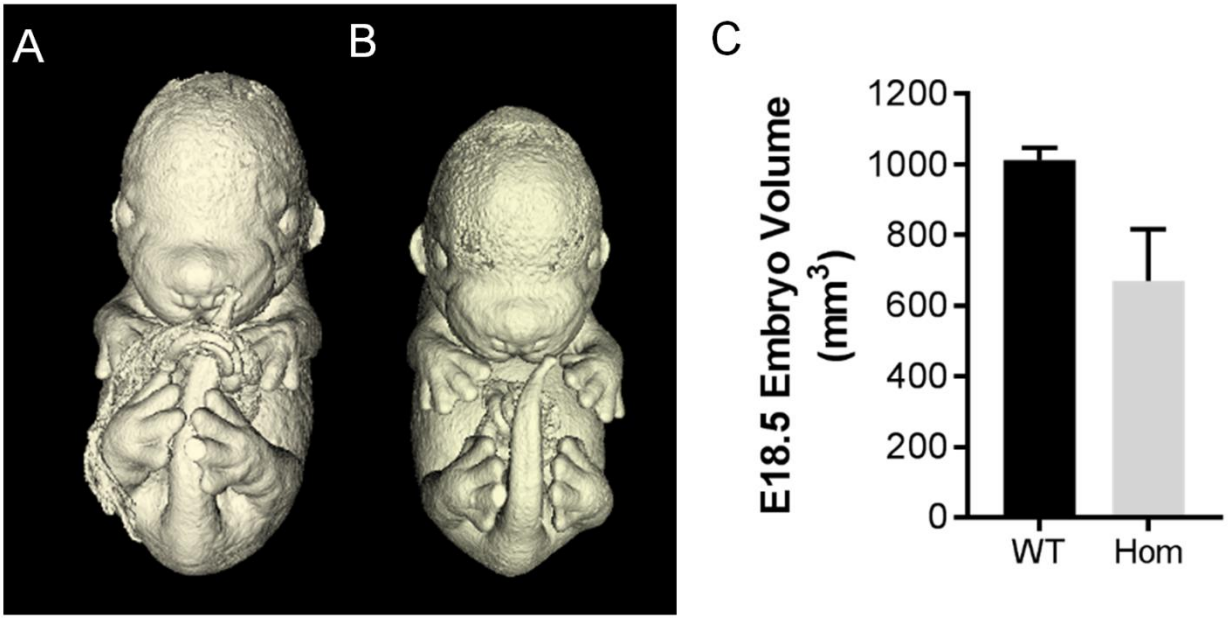

Figure S3. *Otud6b* deficiency reduces mouse embryo volume. (A & B) Representative μCT images of E18.5 wild-type (A) and *Otud6b*$^{tm1b/tm1}$ (B) embryos. **(C)** Analysis of E18.5 wild-type (WT) and *Otud6b*$^{tm1b/tm1b}$ knockout embryo (Hom) μCT images reveals a reduction in knockout embryo volume (N = 2 for each group).

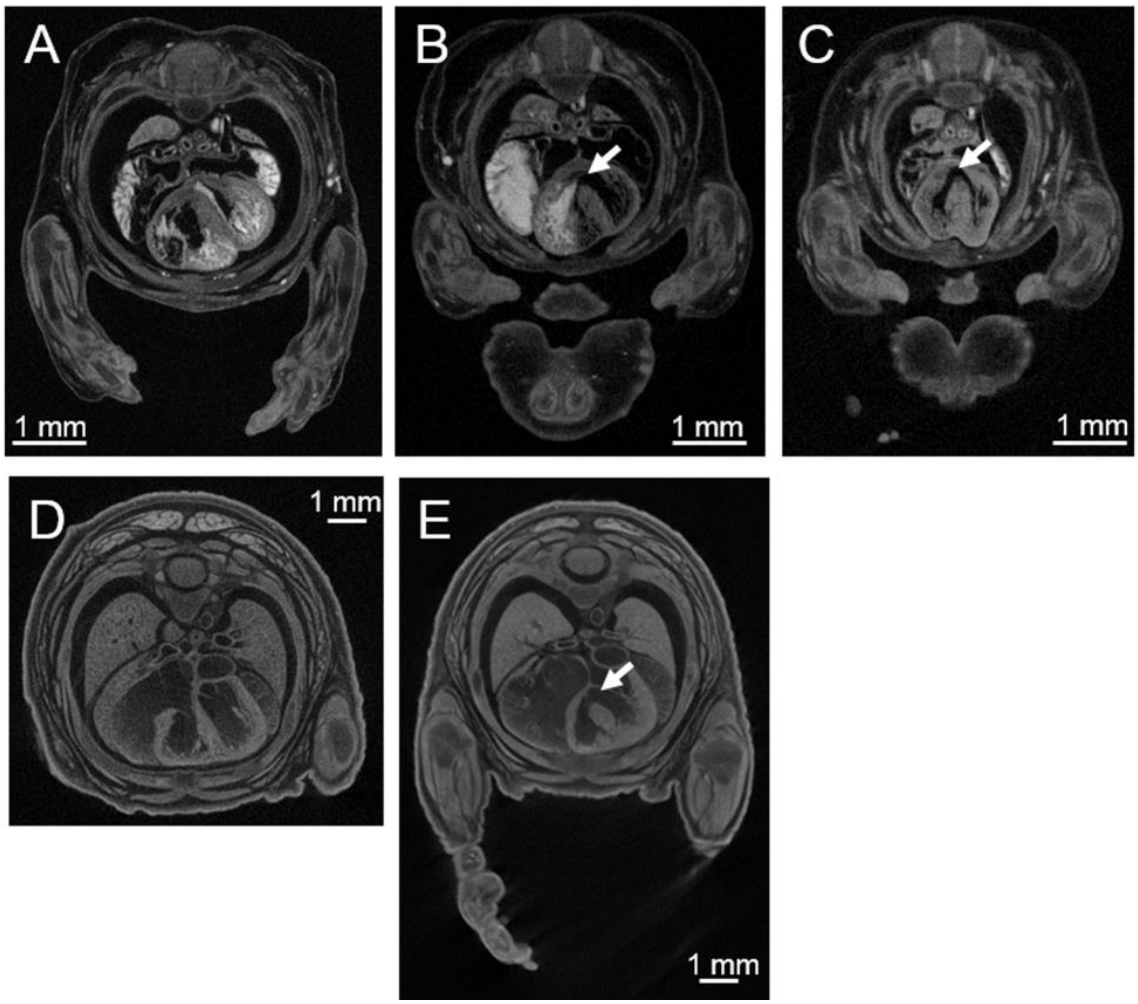

Figure S4. Ventricular septal defects in *Otud6b* knockout embryos. μCT image of E14.5 wild-type **(A)** and *Otud6b*$^{tm1b/tm1b}$ knockout **(B & C)** embryos and E18.5 wild-type **(D)** and *Otud6b*$^{tm1b/tm1b}$ knockout **(E)** embryos. The ventricular septal defect in the *Otud6b*$^{tm1b/tm1b}$ knockout embryo is indicated (arrow).

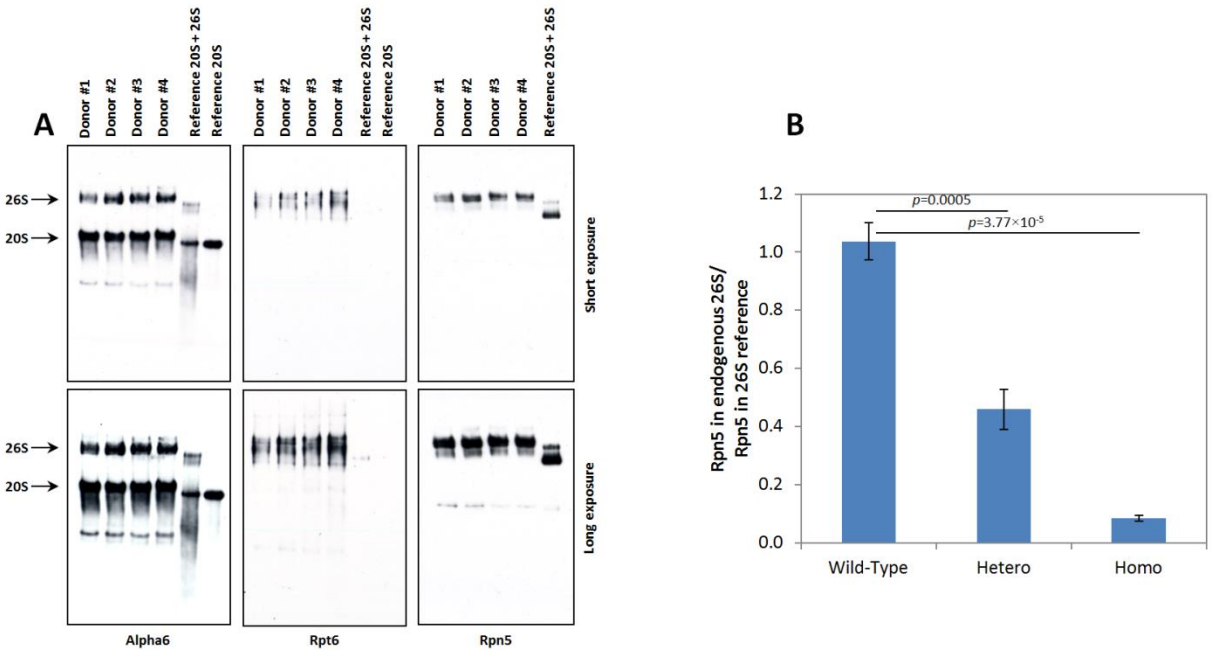

Figure S5. Wild-type *OTUD6B* are more efficient than *OTUD6B* heterozygotes and homozygotes at incorporating the Rpn5 subunit into 26S proteasomes. (A) Forty micrograms of whole-cell extracts of PBMC derived from four healthy blood donors were resolved by native-PAGE and subjected to western-blotting using antibodies specific for Alpha6, Rpt6 and Rpn5, as indicated. Two exposure times (short, upper panel and long, lower panel) are shown. **(B)** The intensity of the Rpn5 bands located in the region of 26S proteasomes from the native-PAGE experiments depicted in Figures 5 A and S5 A were quantified by densitometry (ImageJ 1.48v) and normalized to the 26S reference (200 ng) of the same gel. Shown is the ratio of Rpn5 in endogenous 26S proteasome/Rpn5 in 26S reference for the wild-type *OTUD6B* subjects as well as for subjects heterozygous or homozygous for the c.469_473delTTAAC *OTUD6B* deletion.

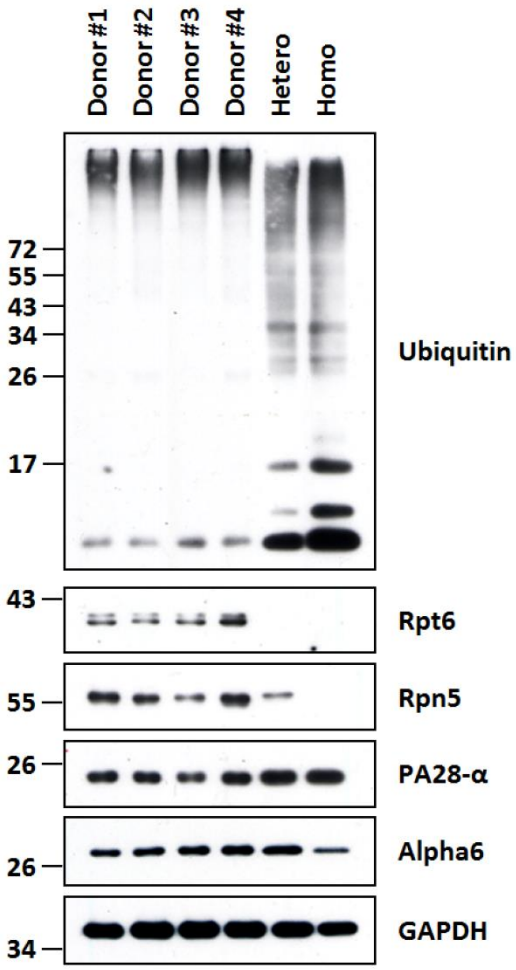

Figure S6. Both *OTUD6B* heterozygotes and homozygotes show proteasome impairment as well as disturbed protein homeostasis. Ten micrograms of protein lysates of PBMC derived from four healthy blood donors or from subjects with the hetero or homo c.469_473delTTAAC *OTUD6B* deletion were separated by SDS-PAGE prior to western-blotting using antibodies specific for ubiquitin (DAKO), Rpt6 (clone p45-110, Enzo Life Sciences), Rpn5 (clone H-3, Santa Cruz Biotechnology, Inc.), PA28-α (K232/1, laboratory stock) and Alpha6 (clone MCP20, Enzo Life Sciences), as indicated. Equal protein loading between samples was ensured by probing the membrane with anti-GAPDH antibody.

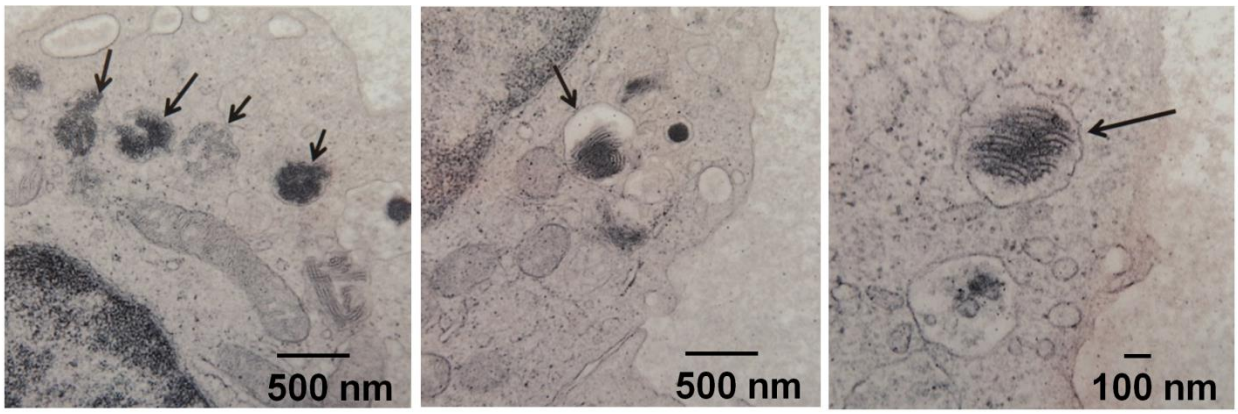

Figure S7. Accumulation of abnormal cytoplasmic inclusions in lymphocytes of Subject II-2 from Family 2. Transmission electron microscopy images of lymphocytes showing an accumulation in the cytoplasm of abnormal inclusions with a tubular configuration (arrows).

Table S1. *Otud6b* genotypes observed after birth.

Genotype	No. observed*	No. expected	Test score (χ^2, *P* value)†
Otud6b$^{+/+}$	32	32	
Otud6b$^{tm1b/+}$	63	64	28.14, < 1E-5
Otud6b$^{tm1b/tm1b}$	2	32	

***** Assumes *Otud6b*$^{+/+}$ mice were observed at the expected frequency and a 1:2:1 segregation ratio. † Chi-square goodness-of-fit tests (2 D.F.) tested for statistical differences between the observed and expected number of progeny.